THESIS FOR THE DEGREE OF LICENTIATE OF ENGINEERING

Analysis of Condensable Hydrocarbons in Gasification Processes

Mikael Israelsson

Department of Energy and Environment

CHALMERS UNIVERSITY OF TECHNOLOGY

Gothenburg, Sweden 2014

Analysis of Condensable Hydrocarbons in Gasification Processes

Mikael Israelsson

Department of Energy and Environment
Division of Energy Technology

Chalmers University of Technology
SE-412 96 Gothenburg
Sweden
Telephone + 46 (0)31-772 1000

Printed in Sweden
Chalmers Reproservice

Gothenburg 2014

Analysis of Condensable Hydrocarbons in Gasification Processes

Mikael Israelsson
Division of Energy Technology
Chalmers University of Technology
SE-412 96 Gothenburg (Sweden)

Abstract

Biomass gasification is a primary process step for the production of biofuels. The gasification process produces a combustible gas mixture which consists of a wide range of species from permanent gases to condensable hydrocarbons, collectively known as tar. Tar starts to condense at temperatures around 350°C, causing blockage and fouling of downstream equipment such as heat exchangers. The conventional means of gas cleaning are based on various methods of scrubbing to remove all condensable species, including steam. However, these systems suffer losses in terms of low heat recovery, and the chemical energy of the tar is removed from the product, thus lowering the overall efficiency. An alternative to scrubbing is catalytic reforming of the produced tar into light gas species by means of primary or secondary measures. The benefit of tar reforming is that the energy content of the tar is retained in the produced gas. Furthermore, if the tar is reduced to low enough levels, the heat recovery of the process can be increased.

This study investigates the concepts of primary and secondary measures by introducing a catalytic material directly into the Chalmers DFB gasifier (primary measure) and by utilizing an additional reactor for catalytic reforming of the produced gas (secondary measure). These two concepts differ in terms of operation and cost, as well as in the type of gas that comes into contact with the catalytic material. For the primary measures, the catalytic material is introduced to a newly formed pyrolysis gas, whereas the gas entering the secondary measure equipment has already evolved due to its time in the gasifier. Overall, both concepts resulted in significantly decreased levels of tar. However, the composition of the remaining tar differed between the two concepts, as well as the added amounts of oxygen.

Sufficient quantification of all components of the produced gas is required to evaluate the performance of a gasifier system. However, as the produced gas comprise such a wide range of species, several different measurement techniques are required. This requirement often results in incomplete quantification as the individual measurements have limitations as to which species can be detected. The SPA method for tar measurement was evaluated to determine the detection limits and reproducibility of the method. Species ranging from phenol to coronene were measured with a relative standard deviation well within 10%; however, the light species ranging from benzene to xylene were not sufficiently adsorbed to the employed SPA column.

A high-temperature reactor, for thermal cracking of all gas species into CO, CO_2, H_2, and H_2O, was constructed to measure the total elemental yields of C, H, O, and N in the raw gas.

This measurement allowed a mass balance of the system to be constructed that, combined with the cold gas and tar measurements, was used to obtain information on the yield and possible composition of previously unmeasured condensable species. This group included more than twice the amount of carbon found in the SPA measured tar, which emphasizes the need of quantifying it in standard measurements. The information gained from this type of measurements can be of great value both for choosing and evaluating primary and secondary measures for tar reduction, as well as for the construction of comprehensive reaction schemes for the evolution of tar.

Keywords: Tar, condensable species, SPA, CLR, DFB.

List of Publications Included in the Thesis

I. Fredrik Lind, Mikael Israelsson, Martin Seemann, Henrik Thunman. Manganese oxide as catalyst for tar cleaning of biomass-derived gas. *Journal of biomass and biorefinery*, 2012, 2, (2), pp 133-140.

II. Anton Larsson, Mikael Israelsson, Fredrik Lind, Martin Seemann, Henrik Thunman. Using ilmenite to reduce the tar yield in a dual fluidized bed gasification system. *Energy & Fuels*, 2014, 28, pp 632−2644

III. Mikael Israelsson, Martin Seemann, Henrik Thunman. Assessment of the solid-phase adsorption method for sampling biomass-derived tar in industrial environments. *Energy & Fuels* 2013, 27, pp 7569−7578

IV. Mikael Israelsson, Anton Larsson, Henrik Thunman. Online measurement of elemental yields, oxygen transport, condensable compounds, and heating values in gasification systems. *Energy & Fuels*, accepted for publishing.

Mikael Israelsson is the principal author of papers III and IV. Fredrik Lind and Anton Larsson are the principal authors of papers I and II respectively, Mikael Israelsson contributed with tar analysis, evaluation and editing to both papers. Assistant Professor Martin Seemann is assistant academic supervisor and participated in the experimental work, as well as contributed ideas and editorial support. Professor Henrik Thunman is principal academic supervisor and has contributed ideas, discussions and editorial comments to all papers.

Publications not Included in the Thesis

- Nicolas Berguerand, Fredrik Lind, Mikael Israelsson, Martin Seemann, Serge Biollaz, Henrik Thunman. Use of nickel oxide as a catalyst for tar elimination in a chemical–looping reforming reactor operated with biomass producer gas. *Ind. Eng. Chem. Res.*, 2012, 51 (51), pp 16610-16616.

Acknowledgment

I would like to thank my main supervisor Henrik Thunman for always taking the time to discuss various aspects of my work and contributing with ideas. Martin Seemann and Fredrik Lind, thank you for your support throughout this work and for assisting in the experimental and writing processes.

I also thank everyone in the gasification group for contributing to an excellent working atmosphere during this time. Thank you Anton Larsson, Jelena Marinkovic and Teresa Berdugo Vilches for your help with the measurements and the time we shared in the power central. Special thanks to Anton for being a great co-author and for always being willing to discuss various theories, regardless of field.

A big thank you to our research engineers Jessica Bohwalli, Rustan Marberg, Johannes Öhlin, and Ulf Stenman for contributing with ideas and taking the time to help me throughout this work.

Thank you everyone at the division of energy technology for creating a fantastic work environment, and Olivia for being a first-class roommate.

Finally, I would like to thank my family and friends for your support. Last but not least, my beloved Carin, thank you for everything.

This work has been financially supported by E.ON AB, Akademiska Hus, Göteborg Energi AB, Valmet AB (previously Metso Power AB), and the Swedish Energy Agency. The latter part of this work was performed within the Competency Center of the Svenskt Förgasningscentrum (SFC).

Mikael Israelsson, Göteborg 2014

Table of Contents

---

1 - Introduction

The production of biofuels from national biomass resources presents a secure supply of fuel at reduced CO_2 emissions, while maintaining job opportunities in the forest industry. This study focuses on biomass gasification, which is a primary process step for the production of biofuels, in which the fuel undergoes thermochemical conversion to yield a combustible gas. There are currently several process types available for the gasification of biomass, which present large differences in operational temperature, pressure, fuel type and means of generating the heat necessary for conversion [1, 2].

The present study focuses on measurements coupled to indirect, dual fluidized bed (DFB), gasification, wherein part of the fuel is combusted in a circulating fluidized bed (CFB) to generate heat for the gasification of the remaining fuel, Figure (1). The heat is transported from the combustor to the gasifier by means of a bed material which, in combustion processes, is usually comprised of silica sand. However, in DFB gasification, natural ores such as olivine, ilmenite, bauxite or any other economically feasible material are often used[3, 4]. The main benefit of indirect, compared to direct gasification, is that the gas produced will contain less CO_2 and N_2, due to the combustion taking place separately whilst the gasifier is fluidized using only steam. Conversely, the benefits of direct gasification include the ability to operate at higher temperatures and pressures, as only one process vessel is utilized for fuel conversion.

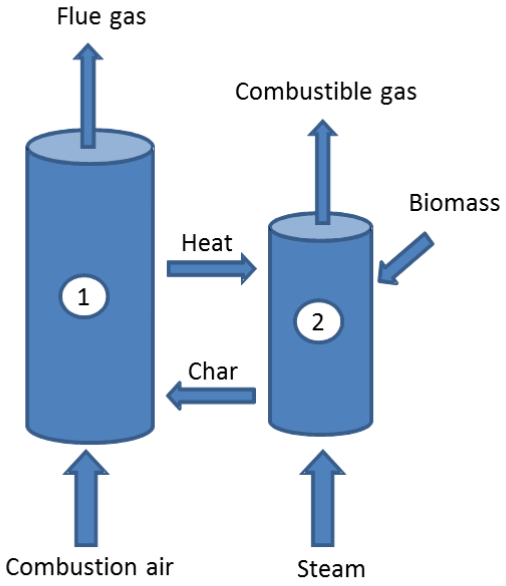

Figure 1: Schematic of the Chalmers DFB gasifier consisting of 1: CFB combustor, 2: gasifier.

With the possible exception of gasification at exceedingly high temperatures, all available gasification techniques produce a raw gas consisting of a broad spectrum of species. This spectrum encompasses species ranging in size from hydrogen and methane to heavy, condensable organic species, commonly referred to as tar[2]. Tar is an unwanted byproduct, which poses an enduring challenge to gasification, as described by Tom Reed (1998, adopted from Milne[2]).

> *"While a great deal of time and money has been spent on biomass gasification in the last two decades, there are very few truly commercial gasifiers, operating without government support or subsidies, day in, day out, generating useful gas from biomass. The typical project starts with new ideas, announcements at meetings, construction of the new gasifier. Then it is found that the gas contains 0.1-10% 'tars.' The rest of the time and money is spent trying to solve this problem. Most of the gasifier projects then quietly disappear. In some cases the cost of cleaning up the experimental site exceeds the cost of the project! Thus 'tars' can be considered the Achilles heel of biomass gasification. In the gasification of coal, a more mature technology, the 'tars' (benzene, toluene, xylene, coal tar) are useful fuels and chemicals. The oxygenated 'tars' from biomass have only minor use. With current environmental and health concerns, we can no longer afford to relegate 'tars' to the nearest dump or stream."*

Tar is a fairly ambiguous term and there are several different definitions. In this work, tar is defined as all organic species with a boiling point above or equal to that of benzene (80°C). Furthermore, the raw gas is divided into permanent gas, or cold gas (comprising species ranging from hydrogen to propane), steam, and condensable species (including tar), which consist of all carbon containing species in the raw gas that are not found in the cold gas.

In line with the quote by Reed, any process, in which the raw gas is further treated for biofuel production, suffers greatly if the raw gas has not been cleaned from tar prior to treatment. If the tar is not sufficiently removed, the remaining tar may condense in pipes and coolers, as well as deactivate catalysts in downstream equipment, causing severe operational difficulties. The different methods available for gas cleaning can be divided into two types; methods that separate the tar from the gas stream, such as scrubbing[5], and methods that reform tar into light gas components[6, 7]. The benefit of the second type is that the energy content of the tar is retained in the gas.

1.1 Primary & Secondary Measures: Gas Cleaning

Scrubbing of the raw gas will, most likely, always be necessary to some extent due to the presence of steam and trace amounts of tar. However, there is still an incentive to pursue reforming methods as they can both increase the overall efficiency of the process and decrease the demand on the scrubber. Consequently, the complexity, and cost, of the reforming method employed is determined by the potential gains in terms of efficiency and gas cleaning.

The different methods for reforming the raw gas can be divided into primary and secondary measures and two different methods are investigated in Papers 1 and 2. Primary measures are implemented within the gasifier while secondary measures require auxiliary equipment. In general, primary measures are cheaper and are, therefore, often implemented as a first step towards decreasing the tar content to acceptable levels. However, if the primary measures are unsuccessful, secondary methods can be considered provided that the potential gain outweighs the cost.

Paper 2 describes the implementation of ilmenite ore as part of the bed material in the Chalmers 2-4MW DFB gasifier. The active material is circulated together with the sand and transports heat to the gasifier, where it catalytically supports the conversion of tar and condensable species into lighter gases. The activity of the material decreases as it resides in the gasifier due to the deactivation by sulfur and carbon deposits on the active surfaces. When the bed material enters the boiler, it is regenerated and heated as the deposits are combusted before the material re-enters the gasifier. An important factor concerning active materials is their ability to transport oxygen from oxidizing to reducing environments *via* metallic species such as iron. This phenomenon is exploited in certain technologies, like chemical looping combustion (CLC)[8], but should be suppressed in gasification processes as the transported oxygen combusts the product gas, thus reducing the efficiency. However, the required bed material flow is governed by the heat demand of the gasifier, which results in a given oxygen transport for a given bed material.

When a catalytic material is used as a secondary measure for raw gas cleaning (Paper 1), the produced raw gas is introduced to a secondary process vessel containing the active material. Several different approaches are possible for secondary tar cleaning, such as single fluidized beds and packed beds with a wide range of active materials[6]. Furthermore, secondary measures, which do not utilize catalytic materials are possible, such as thermal cracking. In this work, the secondary vessel is a chemical looping reformer (CLR)[7], which is a dual fluidized bed containing manganese ore. The dual beds operate in a way similar to the combustor and gasifier. The catalyst transports heat and oxygen to the reformer, where it reforms tar and condensable species, after which it is subsequently regenerated and heated in the air reactor. The circulation rate of the bed material is determined by the deactivation and the heat transport necessary to sustain the endothermic reactions of the reformer. However, as the heat required for gasification is supplied within the gasifier, a lower circulation rate can be obtained in the CLR, which results in a lower level of oxygen transport.

The main benefits of secondary measures for tar reduction include the ability to control, to some extent, the oxygen transport and the possibility of separating the active material from the ash in the fuel. Furthermore, it is likely that higher levels of tar conversion will be reached as the process can be optimized without taking the gasifier operation into consideration. On the other hand, the need for auxiliary equipment increases significantly the complexity and cost of the overall process. A clear understanding of the process performance is needed to decide what type of measure is required for a satisfactory level of tar reduction. Consequently, the ability to measure and/or predict the tar yield in the raw gas offers valuable input for the design of the gas cleaning equipment.

1.2 Quantification of Fuel Conversion

Reliable measurements of a majority of the in- and outgoing streams of a gasifier are needed to establish a satisfactory mass balance. This requirement puts high demands on measurements performed on DFB units, as the flow of unconverted fuel, leaving to the combustor is difficult to measure directly. However, similar difficulties are present in direct gasification as unconverted fuel can accumulate or exit with the gas and ash removal streams. As a result, the raw gas stream needs to be completely quantified in terms of the total elemental flows, cold gas, tar, and steam content to accurately describe the fuel conversion, efficiency, tar yield and other parameters of interest. Figure 2 depicts the steam-free raw gas in terms of cold gas, tar, and the total elemental yields of C, H, O, and N. Other elements, such as S and Cl, could also be included in the total elemental yields; however, the present study focuses on streams that are large enough to be of relevance to the overall mass balance.

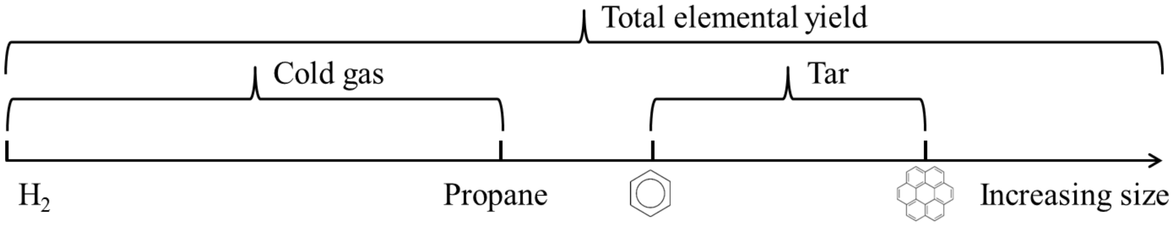

Figure 2: Identified segments of the raw gas spectrum.

The permanent gases, often referred to as cold gas, are cleaned from tar and steam using a gas conditioning system after which the dried gas is quantified using a micro-GC. As a result, the amount of species present in the cold gas is restricted by the analysis equipment, as well as the gas conditioning system. In this work, the cold gas contains species ranging from hydrogen to propane. Furthermore, the total flows of the cold gas components are quantified by adding a known flow of helium to the steam used to fluidize the gasifier. Due to the difficulties of online steam measurements caused by particles and condensing tar species, the steam content of the raw gas is often estimated through condensation, using the gas conditioning system. However, this estimation is time consuming and difficult to perform accurately as stable operation is required.

There are currently several methods for both off- and online measurement of tar[9-15]. The majority of the online methods are more suitable for monitoring trends in the tar amount as they do not differentiate between the different tar species. The two main offline methods, European tar protocol[14] and solid phase adsorption (SPA)[15-17], are better suited for mass balance purposes as they allow the identification of individual species. These two methods mainly differ in terms of sampling; the European tar protocol is a cold trapping method, whereby tar is condensed in a series of impinger bottles filled with a solvent. In comparison, for the SPA method, a small amount of raw gas is extracted through a column containing an amine which adsorbs the tar. The tar is subsequently removed from the column through eluation, using a solvent. The dissolved tar is then analyzed using a GC-FID or GC-MS for both mentioned methods.

In this study, the SPA method was chosen for tar analysis on the grounds of it requiring less time and equipment for sample collection. Furthermore, the ability to collect several samples simultaneously allows determination of the reproducibility. The accuracy, reproducibility and measurable species of the SPA method was investigated in Paper 3 to evaluate its suitability for monitoring tar behavior in large scale systems.

The use of a gas-conditioning system for analysis of the cold gas, together with the SPA method for tar analysis, enables the quantification and identification of a majority of the carbon containing species produced in the raw gas. Unfortunately, as both measurements are restricted in terms of which species they can measure, certain species in the raw gas will remain unmeasured. As previously mentioned, these species include GC-undetectable and gravimetric tar, soot and light gas species in the range between propane and benzene.

To resolve the issues linked to incomplete quantification, Neves *et al.*[18] have proposed a method for the quantification of C, H, O, and N in the raw gas that involves combusting the gas prior to the analysis. This method enables determinations of the total elemental flows in the raw gas using comparatively simple equipment, such as a NDIR system or micro-GC. The developed system was successfully used to measure the raw gas from the Chalmers 2-4–MW DFB gasifier. Furthermore, the performed experiments raised the possibility of obtaining even higher levels of accuracy using this type of measurement. Paper 4 investigates the possibility of improving the method proposed by Neves *et al.* by means of thermal cracking of the raw gas. Heating the raw gas to 1700°C induces fast decomposition of complex species into CO, CO_2, H_2O and H_2 with very low soot yields. The main benefit of thermal cracking, compared to combustion, is that all uncertainties concerning the reactant gas in terms of flow and composition are avoided. Furthermore, the reformed gas is not diluted by the nitrogen present in the combustion air. The fact that nitrogen is not added also allows the performed nitrogen measurement to be used to detect possible leaks. The resulting gas mixture was analyzed using a micro-GC to obtain the total elemental flows of C, H, O, and N in the raw gas. This allowed an indirect determination of the amount of unidentified condensable species as the elemental flows of the raw gas were compared to the elemental flows of the cold gas and SPA-detectable tar.

The ability to use the high temperature reactor (HTR) to completely quantify the raw gas allows the mass balance of the gasifier to be fulfilled. As a result, additional parameters such as the total fuel conversion, char conversion and oxygen transport in DFB systems can be determined. Furthermore, the energy balance of the system can be refined to estimate the energy content of the condensable species, in addition to the heating value of the raw gas. This provides valuable information on which actions can be motivated in terms of primary and secondary measures for tar cleaning.

1.3 Aim and Scope

The aim of this thesis is to identify and develop the tools necessary to describe the evolution of tar, while taking into account the effects of other, condensable and cold gas, species. The thesis encompasses the concept of tar formation, evolution and destruction in indirect biomass gasification systems. Papers 1 and 2 investigate the use of catalytic materials to reduce the tar levels of the produced raw gas. However, they also show the importance of comprehensive and accurate measurements to allow any conclusions to be drawn from the experiments. Paper 3 presents an assessment of the SPA method for tar quantification with the aim to determine its detection limits and accuracy. Similarly, the reactor used in Paper 4 was designed to quantify the total elemental flows of the raw gas. The reactor performance was experimentally validated and subsequently evaluated using the Chalmers DFB gasifier.

2 - Theory

2.1 Tar Mechanisms

Tar is formed during the fuel pyrolysis and subsequently matures according to Figure 3 depending on the surrounding conditions.

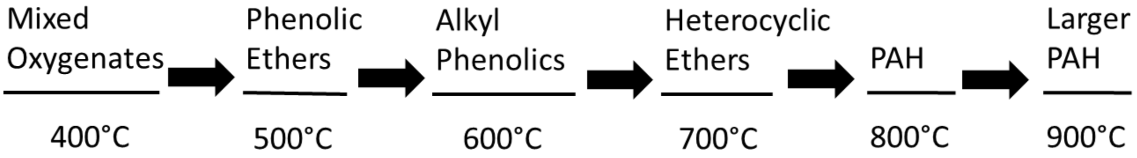

Figure 3: Tar maturation scheme proposed by Elliott (1988), adopted from Milne et al.[2].

The scheme depicted in Figure 3 offers valuable insights concerning the effects of temperature on tar maturation. However, more elaborate schemes are required to construct a useful model for tar evolution. Numerous studies have been performed to model the reactivity of tar[19-22], based on experiments utilizing single tar species[23-25] and synthetic mixtures, as well as various types of biomass[26, 27]. Tar is often described using a small set of model components or groups[19, 22, 28], for example, Corella *et al*. constructed a model based on benzene, 1-ring compounds, naphthalene, 2-ring compounds, 3 & 4-ring compounds and phenolic compounds. Depending on the reactions included in the model, this choice of groups may limit the tar evolution, thus only allowing the tar to decompose into gas or be rearranged into other species. As a result, the contributions of light gas species, soot and GC-undetectable tar[29] to the total tar levels are disregarded. Unsaturated, light hydrocarbons can form or add to the structure of already existing aromatic species *via* the Diels-Alder reaction (R1) followed by dehydrogenation[30-32], or the HACA mechanism (R2)[20, 31, 33]. Furthermore, the decay of GC-undetectable or gravimetric tar might also yield measureable tar species.

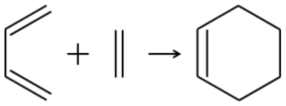

(R1)

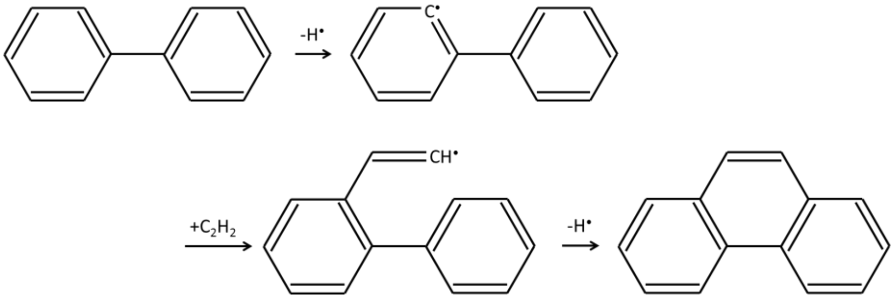

(R2)

GC-undetectable and gravimetric tar species are generally referred to as being very heavy, which implies that they are comprised of several aromatic rings in a soot-like structure, resulting in low H/C-ratios (<0.5). Fuentes-Cano *et al.*[31] performed measurements wherein they determined the elemental composition of the gravimetric tar fraction for temperatures in the range of 600-900°C, resulting in corresponding H/C-ratios ranging from roughly 1.5-1.2. The determined ratios are significantly higher than those expected from soot-like species and are similar to the H/C-ratio of the fuel employed, 1.7. This fact suggests that the collected sample consists of unconverted fuel fragments or primary tar components (Fig. 3). Regardless of the true nature of the gravimetric tar, it is plausible that its decomposition could generate both GC-detectable tar and gas species.

Soot is often considered to consist primarily of carbon, therefore, steam gasification of soot is assumed to yield only CO and H_2. This assumption is probably accurate in many applications; however, pyrolysis experiments performed on soot from pine combustion[33] resulted in a weight loss of 27% at 400°C, consisting of aromatic tar species. In conclusion, if significant levels of gravimetric tar, light hydrocarbons and soot are generated, the effects of these groups on the measureable tar should be considered. One somewhat reoccurring trend in literature that supports the possibility of hidden source terms for tar is an optimum temperature for maximum tar yield[20, 29, 34]. Scott *et al.*[34] found maximum tar yields at 500°C - 550°C for pyrolysis, this was also measured by Morf *et al.*[20], but was discarded as an outlier as it was not reproduced. A similar trend, but at higher temperature (750°C -800°C), was described by Kiel *et al.*[29]. This initial increase in tar level may not be relevant for processes operating at higher temperatures, but it implies that measureable tar can be generated outside of the primary pyrolysis.

2.2 Primary and Secondary Measures

The two approaches to catalytic gas cleaning reported in Papers 1 and 2 mainly differ in the choice of catalyst and level of oxygen transport. However, one potentially important difference is the level of maturity of the gas as it comes into contact with the catalyst. The gas entering the CLR has already experienced the time/temperature history of the gasifier and is, most likely, significantly different from the newly formed gas that comes into contact with the active bed material of the gasifier. Unfortunately, the tar yield of the CLR relative to the fuel feed was not obtained, as the mass balance of the CLR was not satisfied. Consequently, the two measurements are compared on a basis of as-measured concentrations and composition of the measured tar. In line with Paper 1 the tar spectrum was divided into seven groups, based on size and composition, according to: phenols, benzene, 1-ring aromatic species with branches, naphthalene, 2-ring aromatic species with branches, 3 and 4-ring aromatic species, and unknown components. The selected groups correspond to those used by Corella *et al*. with the exception that unknown species constitute their own group. This grouping system was chosen as it separates the different species both in terms of size and reactivity. Typically, the branched species and phenols are more easily converted than pure aromatic components. Additionally, while the identities of the unknown species are (by definition) unknown, their behavior generally reflects that of the branched species. Therefore, they were placed into their own group to clarify the analysis of the other groups.

2.3 Measurement Techniques

The different measurements and streams associated with the gasifier are shown in Figure 4. The inward flows of fuel, steam, and trace gas (helium) are continuously monitored and controlled[35]. The helium is added to the steam prior to it entering the gasifier to facilitate an even distribution throughout the gasifier. The rotary valve, which introduces fuel to the gasifier, is purged using dried flue gas from the boiler. The amount of flue gas that enters the gasifier is determined based on the level of nitrogen in the cold gas. The bed material flow is determined by the operation of the boiler and is responsible for the transport of heat, unconverted fuel and oxygen between the boiler and gasifier. The CLR, high-temperature reactor (HTR) and gas-conditioning system, for the separation of condensable species, operate on a slip-stream of raw gas.

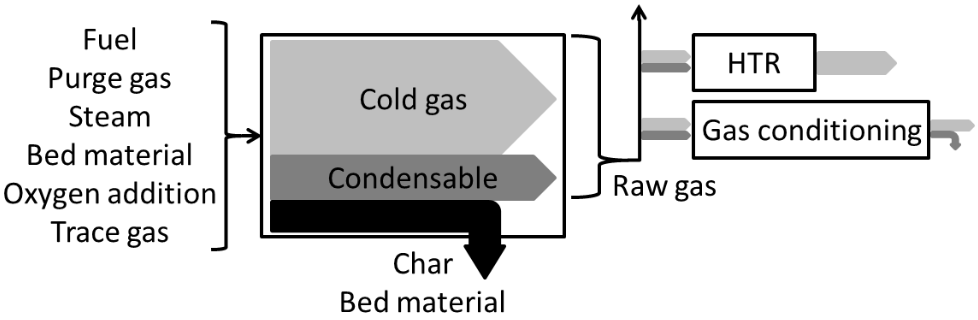

Figure 4: Overview of the flows in the gasifier. HTR, high-temperature reactor.

2.3.1 Tar Analysis

The importance of correct sample acquisition is discussed in Paper 3 together with additional factors that could affect the sampled gas. Regardless of the measurement technique employed, the required slip-stream extraction point, transport tubes and potential dust filters should interfere as little as possible with the gas composition.

As previously stated, the main difference between the SPA method and the European tar protocol is the sample collection procedure. A previous study by Osipovs[16] was conducted to compare the two methods, which yielded similar results for species heavier than xylene. Here, Osipovs used a secondary adsorbent column to improve the measurement of the lighter species benzene, toluene and xylene (BTX); however, the core amount of heavier species was adsorbed in the first column. The sampling time for one SPA sample is roughly 1min, which allows several samples to be collected in rapid succession to detect fluctuations in the gasifier performance. The comparatively long sampling times involved in the tar protocol (i.e., 30−60 min)[15] render it impractical for the determination of rapid fluctuations, which, instead, are represented as a mean value. If the process variations are large, the above can lead to complications in matching the tar data to the measured gas data, as gas measurements are typically carried out at a significantly higher frequency. The long sampling times also make it difficult to compare different sample results from the same experimental point, so as to determine the error of measurement. A faster version of cold trapping developed at the Paul Scherrer Institute in Switzerland (PSI)[36] can be used for resolving variations in the tar output. However, this method still requires the use of a solvent on-site, as well as similar amounts of equipment.

The SPA method, as described by Brage *et al.*, utilizes a 500mg LC-NH2 column for tar adsorption. However, as shown in Paper 3, the reproducibility of the BTX-species is not comparable to that of heavier species such as naphthalene. This has been reported previously[37] and confirmed in unpublished measurements at Chalmers DFB gasifier, using a 500mg LC-NH2 column that also contained active carbon. As a result, all presented values for benzene and toluene within this thesis are to be considered indicative at best.

2.3.2 High-Temperature Reactor

The HTR induces the decomposition of larger molecules into primarily CO, CO_2, H_2, and H_2O, which are more readily measured than the entire raw gas spectrum. The thermal decomposition of various tar components in argon has been thoroughly investigated[23, 24], revealing significant conversion at temperatures in the range of 700°–1000°C and residence times of 5 seconds. Similar measurements, in which soot formation was also determined, were performed using steam with shorter residence times at higher temperatures[25]. Jess[25] achieves complete conversion of naphthalene at 1300°–1400°C, with maximum yields of other tar components and soot at 1100°C and 1250°C, respectively. At 1400°C, the amount of soot decreased, but it was still significant. These findings imply that the temperature and residence times needed for satisfactory conversion to light gases are not dictated by the conversion of tar, but rather by the subsequent gasification of soot. Near-complete conversion of the soot is crucial for this method, as all carbon that remains as soot will cause an error in the mass balance, resulting in a seemingly lower yield of carbon and condensable species.

The HTR system allows on-line measurements of elemental yields through comparison of the molar flow rates of the fuel feed and the gas leaving the HTR, according to:

$$\frac{\dot{n}_{i,HTR\,dry\,gas}}{\dot{n}_{i,fuel}}\left(1 \pm E_{tot,i}\right) = \frac{\dot{n}_{i,HTR\,dry\,gas}\left(1 \pm E_{meas.,i}\right)}{\dot{n}_{i,fuel}\left(1 \pm E_{fuel,i}\right)} = \frac{\sum_j \dot{n}_{j,HTR\,dry\,gas} Y_{i,j}\left(1 \pm \varepsilon_{meas.,j}\right)}{\dot{n}_{i,fuel}\left(1 \pm E_{fuel,i}\right)} \quad (1)$$

where $\dot{n}$ is a molar flow [mol/s], ε describes the degree of error of a specific measurement, and E describes the lumped error of a specific process stream or element. The different elements

(C, H, O and N) are represented by i, while j denotes the various gas components, which include CO, CO_2, H_2, and CH_4. $Y_{i,\,j}$ is the molar content of element i in gas component j [mol/mol]. The measurement error ($\varepsilon_{meas.,j}$) is mainly dependent upon the uncertainty concerning the composition of the calibration gases, which is determined to within 1% relative to the given concentration for all the species. Similar to all measurements wherein a measured parameter is related to the fuel feed, uncertainties related to fuel composition can significantly affect the calculated yields of C, O, and H. Consequently, the fuel feed, moisture content, and composition, as well as the composition of the char need to be determined during the measurements.

In the present study, helium was premixed with the steam feed of the gasifier and used as a trace gas to determine the molar flows of the dried gas according to:

$$\dot{n}_{j,dry\ gas} = \frac{C_{j,dry\ gas}}{C_{He,dry\ gas}} * \dot{n}_{He} \qquad (2)$$

where C is a measured molar concentration [mol/m^3]. The implementation of Eqs. (1) and (2), together with the fuel flow and composition, allows determinations of the carbon-based fuel conversion to raw gas, the char conversion and the oxygen addition in CFB systems, as described in Paper 4.

Operating the HTR system in parallel with a gas-conditioning system permits the acquisition of useful additional information. When the two systems are synchronized, the measurements can be compared to yield indirect measurements of the amount and average composition of condensable species, which consist of all raw gas species that are not found in the cold gas. In combination with known process parameters, such as the fuel and steam feeds, the two systems can be operated (as shown in Figure 5) to monitor the C, H, O, and N molar balances in the gasifier.

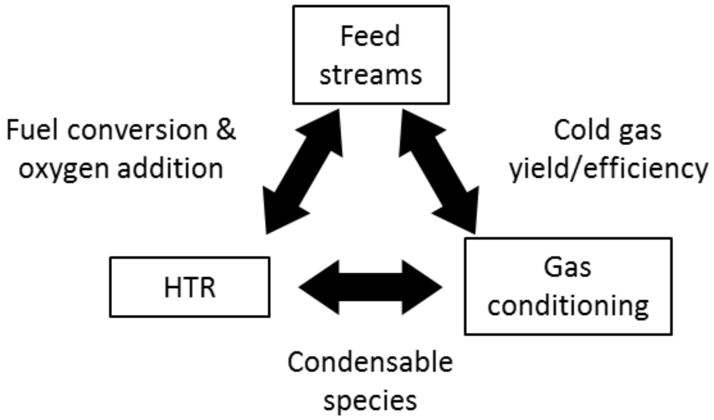

Figure 5: Flow of the data that are included in the mass balance.

Comparison of the data from the gas-conditioning system, G, and the data from the HTR can be done on two levels: with and without SPA analysis of the tar. If the tar measurement is omitted, the comparison is fast and yields information on the amount and average C, O, H composition of all the condensable species (CS) that are not measured by the gas conditioning system, as follows:

$$\dot{n}_{i,CS} = \dot{n}_{i,HTR}(1 \pm \varepsilon_{i,HTR,meas.}) + \dot{n}_{i,HTR,H_2O} - \dot{n}_{i,G}(1 \pm \varepsilon_{i,G,meas.}) - \dot{n}_{i,G,H_2O} \qquad (3)$$

where H_2O represents the condensed steam after the HTR and gas-conditioning system. Errors in the measured amounts of condensate after both systems will affect the determined oxygen and hydrogen content of the condensable species. The errors related to the characterization of the condensable species are also dependent upon the gas measurement. However, as two separate gas measurements are used, i.e., one for the gas-conditioning system and one for the HTR gas, the impact of the analysis error depends on the differences between the two systems in the measured concentrations of a specified component. For instance, if there are low levels of tar and other decomposable components in the raw gas, the difference in the volumetric helium concentration between the two systems will be minor. Similar values for the measured helium concentrations will entail almost identical systematic errors of analysis, provided that the two systems were calibrated using the same gas. Consequently, the resulting total error for helium will be small. Conversely, for large differences in the concentrations of helium, the resulting error will approach that of the calibration gases.

In Paper 4, the accuracy and detection limit of the measurement of the condensable species is estimated by varying the concentrations of all species randomly, assuming normally distributed probabilities, based on the given accuracies of the calibration gases. The main purpose of the HTR system is to quantify product streams that are relevant for the overall mass and heat balances. Therefore, while a low detection limit is desirable, other methods will be more suitable for the quantification and identification of low levels of condensable species[14, 15].

If the tar is measured, using the SPA method, an additional level of comparison is possible. However, the rate of this comparison is low and is dependent upon the performed tar analysis. Subtracting the level of measured tar from the level of condensable species enables the determination of a group of species that was identified by Larsson *et al.*[35]. As they are considered to be semi-volatile, these species are not measured using the SPA method and are too heavy to be measured by the gas-conditioning system. Presumably, this group also contains a fraction of species, ranging from benzene to xylene, which is not completely quantified using the 500 mg of aminopropyl-bonded silica adsorbent in the SPA columns[37]. Regardless of the nature of this group, its quantification allows a deeper understanding of the gas phase chemistry in gasification.

2.3.3 Average Composition of Condensable Species

Both methods for determination of the condensable species, i.e., with or without SPA analysis, require fast and accurate measurements of the steam in the raw gas, to determine with accuracy the oxygen and hydrogen fractions of the indirectly measured components. If the steam is not measured, the condensate terms in Eq. (4) can be omitted. As a result, the average oxygen and hydrogen content of the organic components will include an unknown fraction of H_2O:

$$C_iH_jO_k = C_iH_{j-2x}O_{k-x} + xH_2O \tag{4}$$

The lowest possible hydrogen to carbon ratio of the condensable species can be determined by setting x=k, thereby removing all the oxygen as water. The minimum ratio of hydrogen to carbon, hereinafter referred to as CH_{min}, contains information on the average size of the unknown components, as well as their average heating value:

$$CH_{min} = \frac{j-2*k}{i} \tag{5}$$

A CH_{min} value in the range of 2–4 implies that the condensable mixture mainly consists of alkanes, while CH_{min} values in the range of 0.5–1.0 suggest the presence of aromatic species. However, species with high O/C ratios, such as acrylic acid ($C_3H_4O_2$) and furan (C_4H_4O), have CH_{min} values of 0 and 0.5, respectively. Thus, low CH_{min} values may result from large PAHs, small oxygenated species or both.

2.3.4 Average Energy Content of Condensable Species

The lower heating values (LHV), on a mass basis, vary significantly for different hydrocarbon species, making it challenging to estimate the energy content of the condensable species. As an alternative, the amount of released energy per reacted O_2 molecule needed for combustion [kJ/mole O_2] can be determined for compound A ($C_iH_jO_k$) according to:

$$LHV_{O_2,A} = \frac{\Delta_f H^0_{g,A} - i*\Delta_f H^0_{g,CO_2} - {}^{j}/_{2}*\Delta_f H^0_{g,H_2O}}{i + {}^{j}/_{4} - {}^{k}/_{2}} \tag{6}$$

Implementation of the oxygen-based LHV makes it possible to determine the energy content of the condensable species using only the amount of carbon and the CH_{min} value. Furthermore, it is irrelevant if the “true” component A contains oxygen, i.e., $x \neq k$ in Eq. (5), as this will not affect the amount of oxygen required for combustion. The calculated heating and CH_{min} values of compounds derived from pyrolysis[26] and gasification, as well as those of various alkanes, alkenes, and alcohols are presented in Table 1. Overall, the mean value of the oxygen-based LHV for all three groups is 422.9 kJ/mole O_2, with a standard deviation of 11.7 kJ/moleO_2, or 2.8%, assuming equal amounts of all the species. The accuracy of this approach for determining a heating value is debatable, although it offers a fairly narrow range within which the correct value can be expected. As the condensable species most probably comprise a mixture of compounds, large deviations from the determined mean value are unlikely. Furthermore, the energy contained in the condensable species accounts for roughly 10% of the energy in the fuel[35]. Thus, errors as large as 10% in the oxygen-based LHV will only induce an error of the order of ≤1% in the overall energy balance.

Table 1: Calculated CH$_{min}$ and oxygen-based LHV values for a variety of species present during pyrolysis and gasification.

	CH$_{\mathrm{min}}$	LHV [kJ/mole O$_2$]	Included species
Pyrolysis excluding SPA	0-2.0 (0.79)	418.7-460.3 (436.9)	ethene, acetaldehyde, acetic acid, acetone, acrylic acid, furan, 2-butanone, cyclopentanone, furfural, furfuryl alcohol
SPA tar	0.5-1.25 (0.78)	414.5-431.9 (421.9)	benzene, phenol, toluene, o-cresol, styrene, benzofuran, m/p-xylene, indene, naphthalene, 1-naphthol, 2-methylnaphthalene, dibenzofuran, biphenyl, acenaphthylene, acenaphthene, xanthene, fluorene, phenanthrene, anthracene, fluoranthene, pyrene, triphenylene, coronene
miscellaneous	0.5-3.0 (2.07)	408.1-438.4 (417.0)	ethane, ethanol, propane, propene, propanol, butane, butadiene, butanol, 1,4-butanediol, diacetyl, pentane, 1-pentene, pentanol, n-hexane, cyclohexane, 1-hexanol, heptane, octane, nonane, decane

The calculated average energy content of the condensable species can be combined with that of the dried cold gas to determine the raw gas efficiency according to:

$$\eta_{Raw\ gas} = \frac{\sum \dot{n}_{j,G} * LHV_{j,G} + \left(\dot{n}_{C,CS} + {}^{\dot{n}_{H_{min},CS}}/_{4}\right) * LHV_{O_2,CS}}{\dot{m}_{fuel} * LHV_{fuel}} \tag{7}$$

Similarly, the theoretical raw gas efficiency can be determined by calculating the energy in the converted fraction of the fuel, as Eq. (8).

$$\eta_{Raw\ gas,theor.} = \frac{\dot{m}_{fuel} * LHV_{fuel} - \dot{m}_{char} * LHV_{char}}{\dot{m}_{fuel} * LHV_{fuel}} \tag{8}$$

The resulting efficiency describes the maximum amount of energy in the raw gas that can be recovered from the energy in the fuel. The difference between the above efficiencies can be considered as the enthalpy change within the gasifier due to various reactions, including heat from the bed material that is chemically bound within the raw gas.

The combined energy contents of the dried cold gas and the condensable species can be used together with the total flow of raw gas to determine the LHV [in MJ/Nm^3] of the wet raw gas according to:

$$LHV_{Raw\ gas} = \frac{\sum \dot{n}_{j,G} * LHV_{j,G} + \left(\dot{n}_{C,CS} + {}^{\dot{n}_{H_{min},CS}}/_{4}\right) * LHV_{O_2,CS}}{\dot{V}_{Raw\ gas}} \tag{9}$$

Where $\dot{V}$ is the total volumetric flow of the raw gas [in Nm^3/s], consisting of the cold gas flow, as measured by the gas-conditioning system, the steam flow, determined using the mass balance, and the flow of condensable species, which are assumed to be free of oxygen. Furthermore, it is assumed that the average tar molecule contains six carbon atoms. However, this assumption is of little relevance, as the contribution to the total flow is minor.

The LHV of the raw gas, determined using Eq. (9), requires input data (Figure 5). However, if a gas-conditioning system is not available, the data obtained using only the HTR can be used to determine equivalent LHVs. As an example, the methane-equivalent raw gas LHV is determined by rearranging the gas composition that exits the HTR into CH_4, H_2O, and CO_2. Although the choice of equivalent species is dependent upon the process type, the equivalent LHV nevertheless presents a simple means for process monitoring and control.

3 - Experimental

3.1 Gasifier and Measurement Systems

The gasifier measurements were performed in the Chalmers 2-4–MWth DFB gasifier, depicted in Figure 6. Here, the unconverted fuel from the gasifier is combusted together with additional fuel and the bed material in the CFB boiler (1). The hot bed material is separated from the flue gas in a cyclone (2) after which it enters the particle distributor (4). The flue gas exits at the top of the cyclone and continues towards a series of heat exchangers (3). When the system is operated as a boiler, the bed material exits the particle distributor and returns directly to the boiler. When the system is operated as a DFB gasifier, the hot bed material flow is redirected to the gasifier (5), where it provides the heat necessary for gasification reactions. The cooled bed material exits the gasifier together with the unconverted fuel and char and subsequently enters the boiler. Two separate fuel feeding systems (6) are used for the boiler and gasifier. The produced raw gas, exiting the gasifier, is transported to the boiler for combustion. All performed gas measurements are performed on a slip-stream of gas which is extracted from the sample collection point of the raw gas channel (x).

During measurements, the gasifier is fluidized using steam with a known amount of helium, usually at 20–50 Nl/min, to allow the quantification of gaseous species[35]. The helium is added to the steam prior to it entering the gasifier to facilitate an even distribution throughout the gasifier. The resulting volumetric fraction of helium in the raw gas is around 0.5-1.0%. The gasifier is operated with wood pellets at 1-2kPa sub-atmospheric pressure and temperatures of around 820°C.

The instrumental setup for gas analysis after the HTR is depicted in the left panel of Figure 7. Raw gas (1) is continuously sampled through a heated ceramic filter (2), which is maintained at 350°C and used to remove particles from the gas before it enters the HTR (3). Samples for the SPA analysis are collected directly at the outlet of the HTR (4), as described in Paper 3, to determine the degree of reformation of the SPA-detectable tar fraction. The gas flow is cooled and steam is condensed in a Peltier cooler (5), after which the aerosols are separated using a filter (6). The dry gas is passed through a pump (7) and a flow meter (8) before reaching the micro-GC (9).

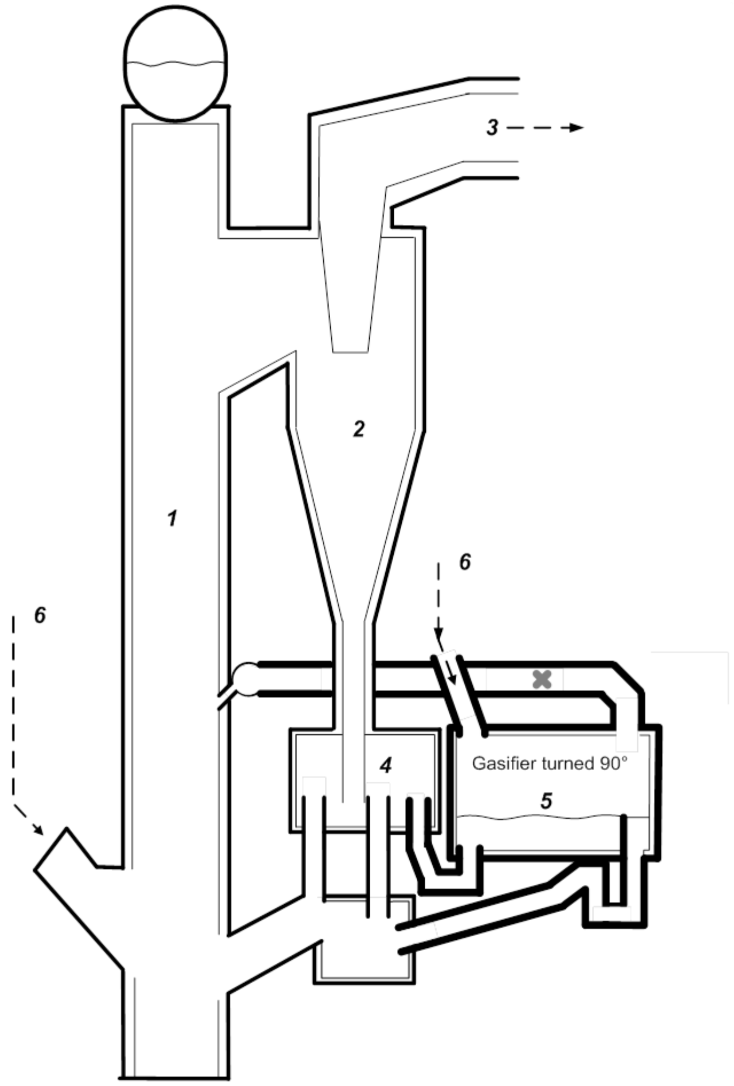

Figure 6: Schematic of the Chalmers DFB gasifier system containing 1: CFB boiler, 2: cyclone, 3: flue gas path, 4: particle distributor, 5: gasifier, 6: fuel feeding systems.

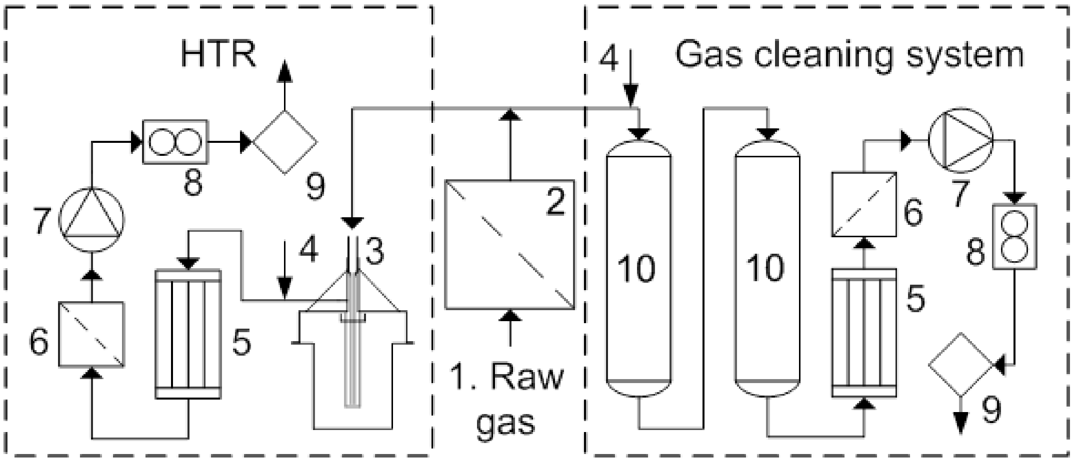

Figure 7: Schematics of the HTR system (left) and the gas-cleaning system (right). The different components are 1: raw gas from gasifier; 2: ceramic filter; 3: HTR; 4: SPA sampling point; 5: Peltier cooler; 6: filter; 7: gas pump; 8: flow meter; 9: micro-GC; 10: cooler.

Cold gas measurements are performed on the untreated raw gas, using the gas-cleaning system (right panel in Figure 7) to determine the dry raw gas composition, concentration of steam, and amount of tar. SPA samples (4) are collected directly after the ceramic filter (2), after which the gas is quenched with isopropanol in two coolers (10), to condense the tar and steam. The gas is further cooled in a Peltier cooler (5), after which it passes through a wool filter (6) to separate the aerosols, a pump (7) and a flow meter (8), before being analyzed in the micro-GC and NDIR instrument (9).

The SPA sampling point (4) of the gas cleaning system was constructed as depicted in the left panel of Figure 8. During measurements, roughly 2 Nl/min of dry raw gas is transported through a heated gas line (350°C), followed by a volume that is heated to the same temperature before reaching the quenching point. The heated volume (350°C) is equipped with a septum mounted a short distance from the wall to avoid melting, which serves as the entry point for the sample syringe. The SPA samples are collected by attaching an SPA column to a 100-ml syringe *via* a universal tube connector, inserting the needle (1.2*50 mm) into the hot gas flow *via* the septum, and extracting 100 ml of gas through the column using the syringe. The remaining raw gas continues through the quench, after which it is cooled and dried before it reaches the online gas analysis equipment. The relatively small flow of gas and the positioning of the quench were selected to ensure a strong response in the N_2 and O_2 concentrations if a leakage should occur during sampling.

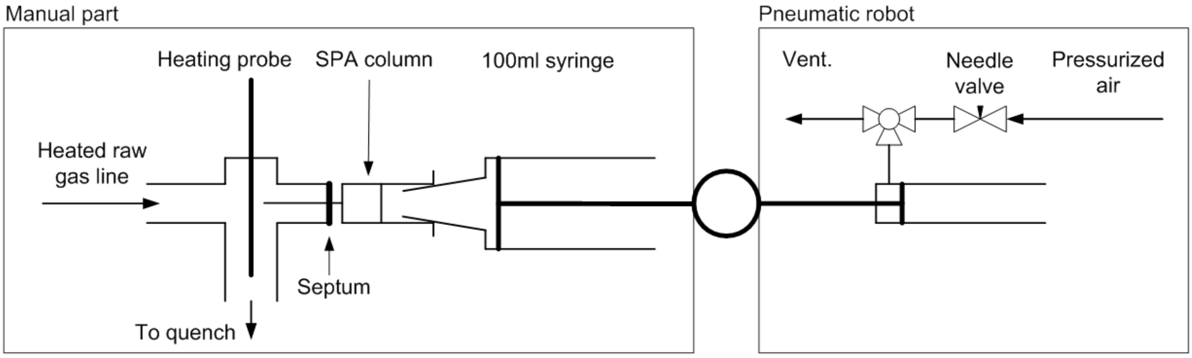

Figure 8: Left panel: SPA sample point, SPA column, and manual part of the extraction device. Right panel: pneumatic robot for consistent sample extraction.

The 100-ml syringe is operated by a pneumatic robot during sample extraction, to allow reproducible sampling (right panel, Fig. 8). The robot consists of a pneumatic cylinder, connected to the syringe, which is filled with pressurized air at a flow rate regulated by a needle valve. This flow rate was calibrated to allow sample extraction times of 1 minute. After collection of a sample, the pressure in the cylinder is released. If a blockage in the needle resulted in the formation of a vacuum, the syringe piston will retract. When this happens the current column is discarded and replaced.

3.2 CLR Reactor System

The CLR reactor system is depicted in Figure 9 together with auxiliary systems, such as analysis equipment and gas supply systems. The employed reactor and analysis systems are thoroughly described elsewhere[7], as well as in Paper 1, and are summarized as follows. Raw gas is introduced to the fuel reactor (FR), which contains a bubbling fluidized bed (indicated in the figure) comprised of silica sand and 23% manganese oxide. During the measurements, the gasifier was operated at bed temperatures of roughly 825-830°C and the CLR was operated at 700 and 800°C. The reformed gas exits at the top of the FR where SPA samples are collected before the gas is conditioned and subsequently analyzed. The air reactor (AR) contains a circulating fluidized bed where the bed material is regenerated by a mixture of air and nitrogen containing between 1-2.2% oxygen. Similarly to the FR, the spent air flow is conditioned and analyzed after exiting the reactor. The FR and AR are separated by two loop seals that prevent the exchange of gas between the reactors and are fluidized using helium. The use of another gas in the seals, such as argon or steam, would contribute to closing the mass balance of the system. Nevertheless, the measurements performed describe clear trends in concentration and composition of the measured tar.

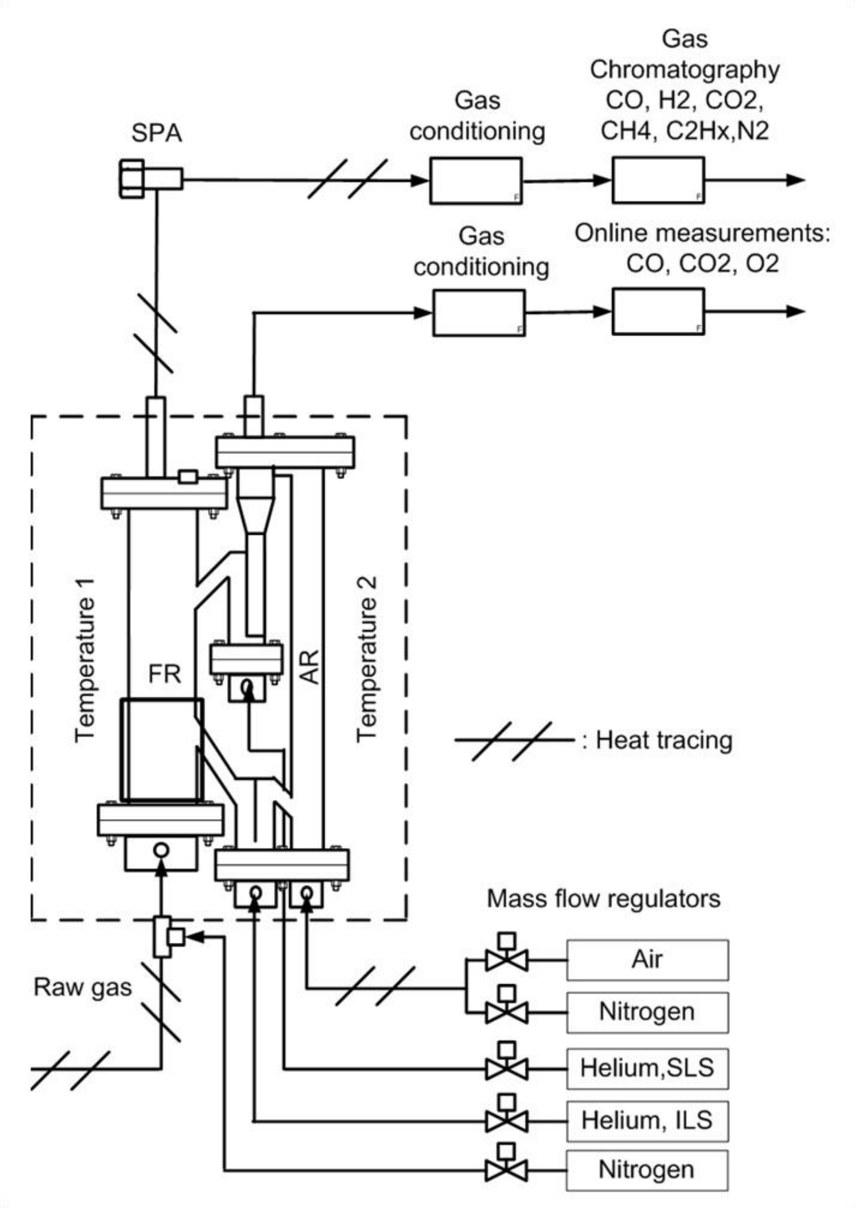

Figure 9: Schematic of the CLR setup.

3.3 Gasifier Operation using Ilmenite

Paper 2 describes the effects of different levels of ilmenite in the bed material (silica sand) on the raw gas produced in the Chalmers DFB system. The gasifier was operated with wood pellets and ilmenite fractions in the range of 0-12% of the bed material. Measurements were performed at high and low levels of fluidization for all investigated levels of ilmenite to discern the effects of increased gas/solid contact. The operating parameters of the gasifier were kept as constant as possible between the different measurements. As a result, the average bed and gas temperatures were between 821-833°C and 788-801°C respectively. However, due to the different levels of fluidization, the steam-to-fuel ratio and average gas residence time were between 0.81-0.82 $kg/kg_{daf\ fuel}$ and 3.87-3.96 s respectively, for low fluidization, and 1.06-1.07 $kg/kg_{daf\ fuel}$ and 3.25-3.36 s for high fluidization. Consequently, the effects of changes in residence time and steam concentration are present in addition to the effects of increased gas-solid contact.

3.4 SPA Methodology

Paper 3 investigates the repeatability of the SPA method, as well as its sensitivity to the effects of incorrect sample collection and subsequent treatment. The measurements performed consisted of six SPA columns each, collected within a period of about 10 minutes. The columns, with the needles still attached, were then sealed and stored in a freezer, to minimize desorption of the more volatile components, after which the columns were eluted within 24 hours of sampling.

The elution of the collected SPA samples in Papers 1, 2, and 3 were performed as described in Paper 3. However, in light of the findings of Paper 3, the elution procedure was re-evaluated and recent measurements have been treated as follows. Only one solvent and internal standard are used; the solvent consists of a mixture of eight parts dichloromethane (DCM), one part isopropanol (IPA), and one part acetonitrile (ACN), the internal standard being 4-ethoxyphenol. During elution, the needle is flushed using 0.5ml of solvent which is deposited on the top of the column, after which a weak flow of nitrogen is used to push the solvent through the column. The internal standard is added directly to the vial, after which an additional 1.5ml of solvent is flushed through the column. This procedure is repeated for all columns, with the exception of flushing the needle, to obtain a control sample, which serves both to evaluate and enhance the elution.

The two gas chromatographs used, the BRUKER GC-430 and GC-450, were operated in the split mode using the SGE 4-mm FocusLiner with fused silica wool, autosamplers, FID detectors, and mid-polar BR-17-ms columns with graphite ferrules. The different species, used to calibrate the gas chromatographs are presented in Paper 3. The temperature ramp, which ranged from 50°C to 350°C, was developed to measure components ranging from benzene to coronene. The injector and detector temperatures were set at 350°C, the split ratio was 20, and the column flow was set to 1 ml/min with helium as the carrier gas. The oven was programed to hold at 50°C for 5 minutes, after which the temperature was increased by 8°C/min until 350°C was reached, where it was held constant for an additional 12.5 minutes to ensure that the entire tar spectrum was retained. The current setup gave a reproducibility level that was within 5% for each chromatograph. During the sample analysis, each sample vial was analyzed three times sequentially, after which the mean values for all peaks were calculated.

A series of eight SPA measurements, each resulting in four to six usable columns depending on the success of the sample collection, was collected for different operating modes of the gasifier to obtain a wide range of tar yields and compositions. These samples were analyzed to determine the behaviors of the heaviest detectable tars, such as coronene. As mentioned above, a temperature of 350°C was maintained in all heated pipes and equipment to avoid condensation. Furthermore, measurements together with visual inspection of the transfer lines were performed to ensure that no condensation had occurred.

To determine the reproducibility of the method, the tar spectrum was divided into the known compounds and groups of unknown species that exited the chromatographic column between two known compounds, being lumped together as one value. The relative standard deviations (%RSD) were calculated for each group and known compound in each SPA measurement and were compared to the corresponding collected mass fractions.

3.5 High-Temperature Reactor System

The high-temperature reactor (Figure 10) consists of a ceramic reactor and oven inside a gas-tight steel casing. Gas, at a temperature of 350°C, is introduced to the top of the reactor *via* a stainless steel adaptor (1). The adaptor is connected to the reactor by a flange (2) using graphite packing to avoid leaks. The other end of the adaptor is connected to an 8-mm alumina (Al_2O_3) tube (3) using a stainless steel fitting with graphite packing, to create a leakage-free joint without breaking the alumina tube. The lower part of the reactor contains a larger 35-mm alumina tube with a closed bottom (4), surrounded by four heating elements (5) (Kanthal Super 1800). The top part of this tube is connected to the reactor ceiling using a pack box (6) with graphite packing. The outer shell of the reactor is composed of stainless steel and is designed to be gas-tight at operational pressures (80-101kPa). In the event of excessive internal gas exchange between the large alumina tube and oven, the gas in the oven can be continuously evacuated to ensure minimal back-mixing into the reactor. During operation, gas is drawn through the adaptor and is heated during its transport to the bottom section *via* the narrow alumina tube. The narrow tube ensures minimal residence times at temperatures that promote high soot yields, but that are too low to support soot gasification. The gas then enters the larger alumina tube and is slowly transported upwards through the high-temperature section of the reactor. The gas exits the reactor *via* an outlet (7) that is positioned 10 cm below the inlet adaptor to avoid excessive convective heating of the upper graphite packing.

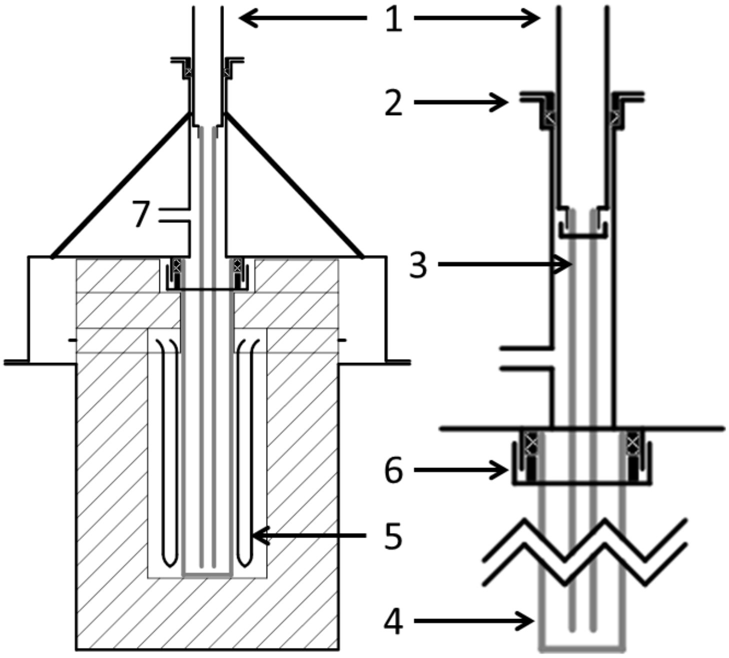

Figure 10: Schematic of the high-temperature reactor (left), with an enlarged image of the connections (right).

3.5.1 HTR Validation Experiments

Synthetic gas HTR measurements were performed to determine the overall degree of conversion and soot formation in the reactor. The start-up procedure for the measurements consisted of initiating a temperature ramp a few hours before operation, to allow the alumina tubes to heat up slowly and, thereby, avoid cracking as a result of thermal expansion. When the operational temperature was reached, the reactor was purged with nitrogen before starting the measurement. Synthetic gas of a known composition was supplied from a gas bottle and mixed with steam to 50%vol before entering the reactor. After the reactor, soot particles were collected in an uncoated diesel particulate filter (DPF), which was maintained at 150°C during operation. The particle-free gas was then cooled to condense the remaining steam before it was analyzed in a micro-GC (Varian CP4900), described elsewhere[35], that was capable of analyzing all the species in the supplied gas. The collected soot was quantified at the end of each measurement by introducing a known flow of air into the system while maintaining the reactor temperature. The oxidation of the system was performed at an initial filter temperature of 150°C, to separate the combustion of remaining gas and soot attached to the pipe walls from the soot captured by the filter. Due to the fast combustion of the soot, the produced CO and CO_2 were measured using an NDIR instrument (Rosemount MLT) to gather data once per second. Once a stable, atmospheric CO_2 background had been obtained, the filter temperature was increased to >500°C, to allow combustion. As a result, the quantified levels of soot should be considered indicative of the total soot yield. Soot formation was determined at temperatures of 1500°C, 1600°C, and 1700°C. Furthermore, the measurement at 1700°C was used to determine the stability, accuracy, and reproducibility of the reactor system.

3.5.2 Applied HTR Measurements

The HTR gasifier measurements were performed in parallel with the gas cleaning system in the Chalmers DFB gasifier according to Figure 7. During the measurement, the gasifier was operated using bauxite to determine aging effects in a separate study. As a result, the system exhibited significant char conversion and oxygen transport between the boiler and gasifier. SPA samples were collected directly after the reactor, to ensure complete conversion of the measureable tar components, and prior to the gas conditioning system to allow analysis of the tar, as well as the undetected condensable species.

The performance of the system was monitored during the measurements to detect possible errors, including air leakages into hot zones, the escape of soot from the HTR, and incorrect synchronization of the equipment. Leakages of air prior to the HTR may be interpreted as oxygen addition, as the leaked air is combusted. Therefore, the He/N_2 ratios of the cold gas and the HTR gas were monitored for deviations. When detected, the amount of leaked air could be determined, and compensated for, by comparing the nitrogen flows of the two systems. The escape of soot from the HTR affects the determined fuel conversion, as well as the yield of condensable compounds. Thus, complete soot conversion needs to be guaranteed for reliable measurements. Incorrect synchronization of the measurements can further complicate the analysis of transient measurements. However, this is rarely a problem as the initiation of helium provides the difference in response time for the two systems.

4 - Results

4.1 Secondary Measures

The measured tar concentrations (g/Nm^3) exiting the gasifier and CLR are depicted in Figures 11 and 12 for operating temperatures of 700 and 800°C, respectively. The measured tar spectrum is divided into phenols, benzene, 1-ring aromatic species with branches, naphthalene, 2-ring aromatic species with branches, 3 and 4-ring aromatic species, and unknown components. However, as previously stated, the measurement of benzene is not reliable and no conclusions can be drawn from its behavior. For both temperatures, the catalytic activity increases as more oxygen is provided in the air reactor. This increase could be caused by higher levels of oxygen transport, resulting in combustion; however, it could also be due to a more extensive regeneration of active surfaces[38]. Overall, the changes in tar composition due to increased severity in terms of temperature and catalyst activity resemble those reported for other materials, such as ilmenite[7]. The concentrations of phenols, branched one and two-ring species, and unknown species decrease throughout Figures 11 and 12 as a result of increased severity. Conversely, the concentrations of naphthalene and three and four-ring species initially increase due to polymerization of other tar species, as well as lighter gas components. At 800°C and 2.2% oxygen in the AR, the three and four-ring species start to decrease and the increase in naphthalene is abating, which indicates that a further decrease can be expected at higher temperatures and levels of catalyst regeneration.

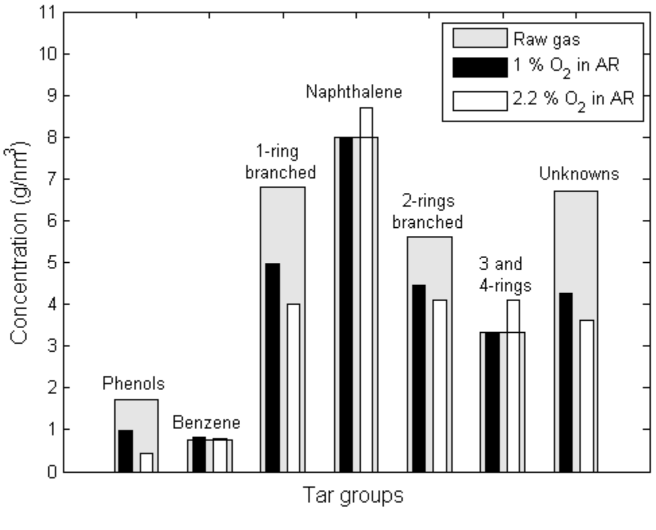

Figure 11: Tar composition for raw gas and reformed gas at 700°C.

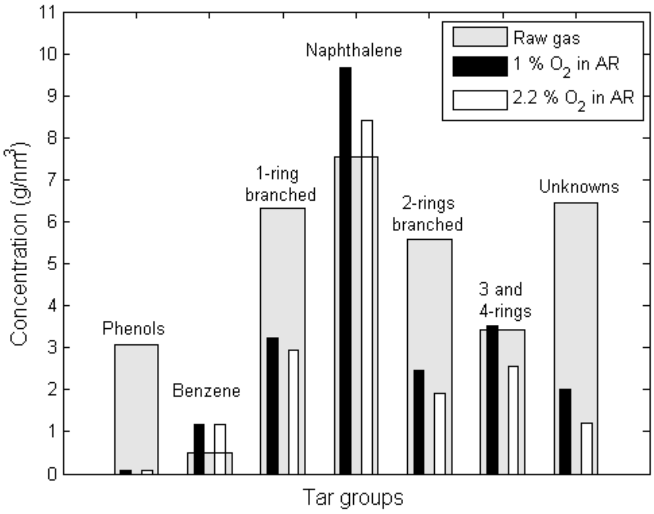

Figure 12: Tar composition for raw gas and reformed gas at 800°C.

4.2 Primary Measures

The gasifier was operated at two different levels of fluidization with ilmenite fractions ranging from zero to 12%. The measured tar concentrations are depicted in Figures 13 and 14, similarly to those of the CLR measurement, for low and high levels of fluidization respectively. The reference cases, with silica sand, are similar to those of the CLR operation. However, the trends in tar composition due to increased severity show little resemblance to the CLR measurements nor do they resemble the expected trends of tar maturation according to Elliott (Figure 3). Instead of shifting the compositions, the measurements at low fluidization (Figure 13) simply decrease the concentrations of all groups, although the phenols seem to be affected to a lesser degree. Furthermore, as seen in Figures 15 and 16, this is not an effect of dilution as the calculated yields of tar species follow the same trend. Presumably, at low levels of fluidization, the degree of contact between gases and solids in the freeboard of the gasifier is limited. Consequently, the decrease in tar is attributed to a high level of contact between the devolatilizing fuel particles and the surrounding bed material. This results in the reformation, or oxidization, of the newly formed primary tar species. The fraction of primary tar, which is able to avoid contact with the active material, subsequently matures in accordance with normal, silica sand, operation of the gasifier.

At higher levels of fluidization (Figure 14), the tar composition differs greatly from the expected trend. The concentrations of both phenols and unknown species are increased, which indicates that the conditions in the gasifier are less severe, since these species are fairly easily reformed. This would suggest that the effects of a shorter residence time outweigh the effects of an increased gas-solid contact. However, as stated in Paper 2, the high level of fluidization also causes higher yields of heavy tar species, which would indicate an increased level of polymerization due to increased severity. There is currently no explanation as to why higher levels of fluidization have this effect on the tar composition. Nevertheless, the measurements performed in the gasifier compared to those of the CLR show that the performance of a catalytic material is strongly dependent on the manner of implementation.

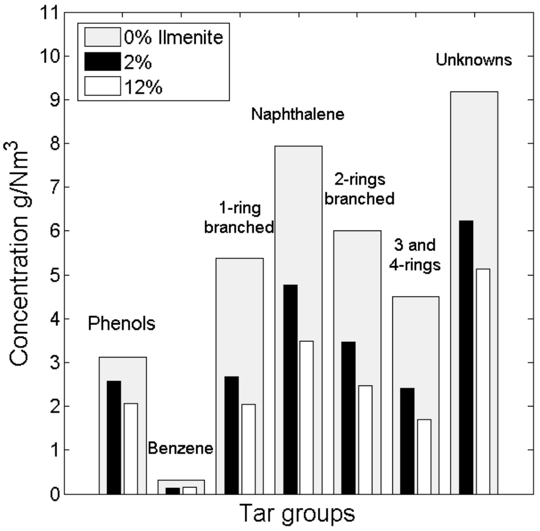

Figure 13: Tar composition for low levels of fluidization with 0-12% ilmenite.

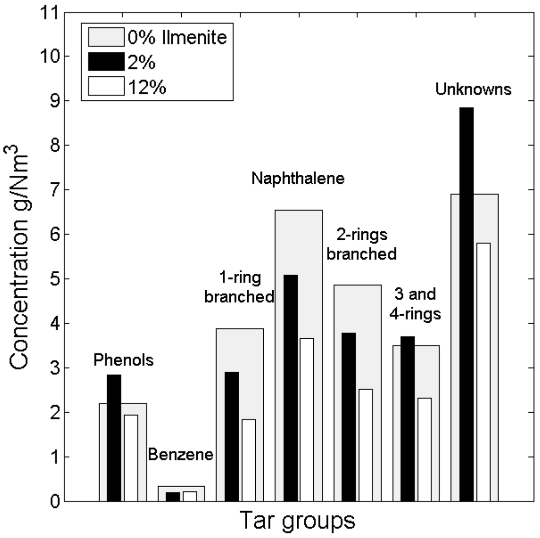

Figure 14: Tar composition for high levels of fluidization with 0-12% ilmenite.

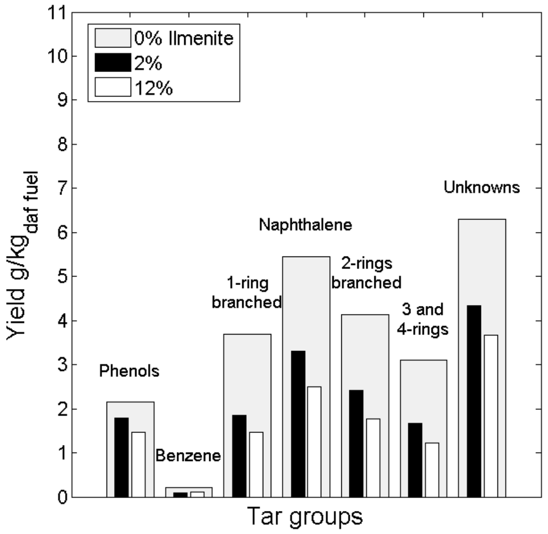

Figure 15: Tar yield [g/kg$_{daf\ fuel}$] for low levels of fluidization with 0-12% ilmenite.

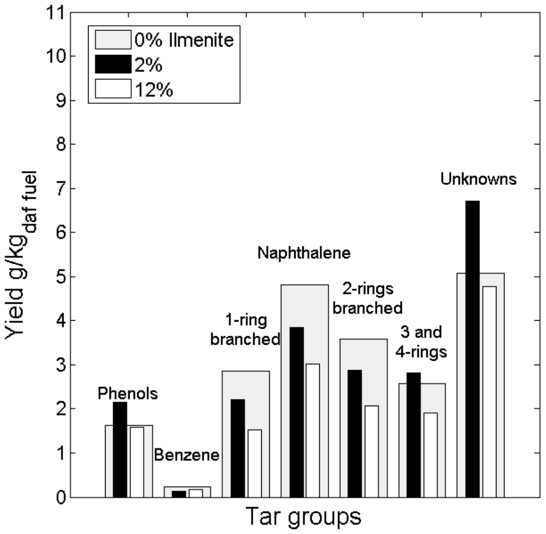

Figure 16: Tar yield [g/kg$_{daf\ fuel}$] for high levels of fluidization with 0-12% ilmenite.

Overall, the reductions in the levels of tar, for CLR operation at 800°C and for low levels of fluidization with 12% ilmenite, are comparable. However, the cost of this reduction, in terms of oxygen transfer differs greatly. Figure 17 shows the molar H/C and O/C-ratios of the measured fractions of CO, CO_2, and H_2 in the cold gas for the gasifier measurements, using 0 and 12% of ilmenite at high and low fluidization, and the CLR measurements at 800°C with 1 and 2.2% oxygen in the air reactor. The solid line, which originates from the point of low fluidization with only silica sand, indicates the change in H/C-ratio as a function of the water-gas-shift reaction. With the exception of high levels of fluidization with silica sand, all points are below the line of the water-gas-shift reaction due to oxygen transport. However, the extent of the oxygen transport is significantly less for the CLR measurements than for the measurements performed in the gasifier, especially at 1% of oxygen in the air reactor. Furthermore, the potential for minimizing the oxygen transport in the CLR is greater than in the gasifier, as it is decoupled from the gasification reactions.

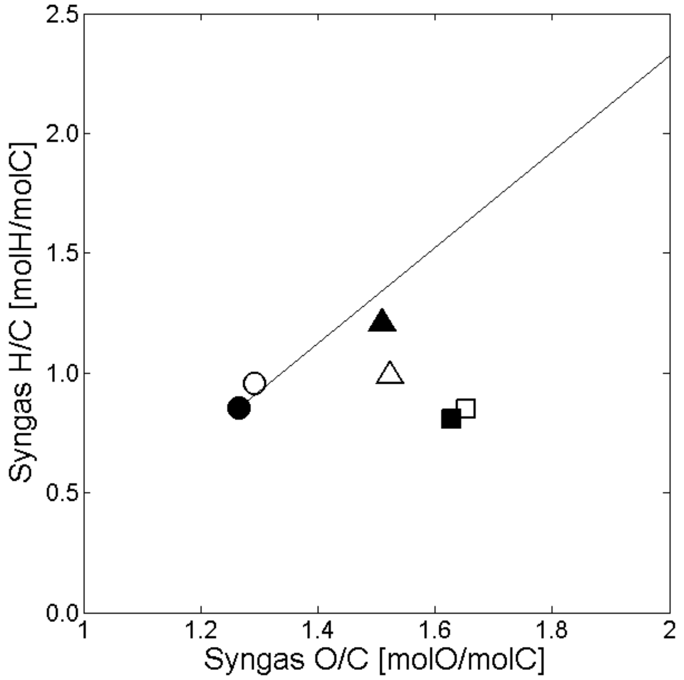

Figure 17: Molar H/C and O/C-ratios of produced syngas species. ● and ○: low and high fluidization with sand respectively, ■ and □: low and high fluidization with ilmenite respectively, ▲ and Δ: CLR with 1 and 2.2% oxygen in the air reactor respectively.

4.3 SPA

The reproducibility of the SPA method was investigated in a series of eight different measurements on the Chalmers DFB gasifier. Figure 18 shows the cumulative mass fractions, of known species and unknown groups, in all measurements compared to the relative standard deviations (%RSD). It is clear that while some species show a high %RSD, the majority of the mass fraction has a %RSD value well within 10%. As shown in Paper 3, the relative standard deviation is noticeably high for the BTX compounds, due to incomplete adsorption. The %RSD was also high for all species that were detected at low concentration, due to them being closer to the detection limit of the analysis method. Moreover, some of the unknown groups, which consist of several species at low concentrations, show a high standard deviation. As discussed previously, the incomplete adsorption of the BTX species was confirmed by employing a new column, which also contained active carbon, in addition to the previously used amino phase. As a result, current measurements utilize the new column to ensure adequate quantification of the lighter tar species. However, these measurements are not included in this thesis.

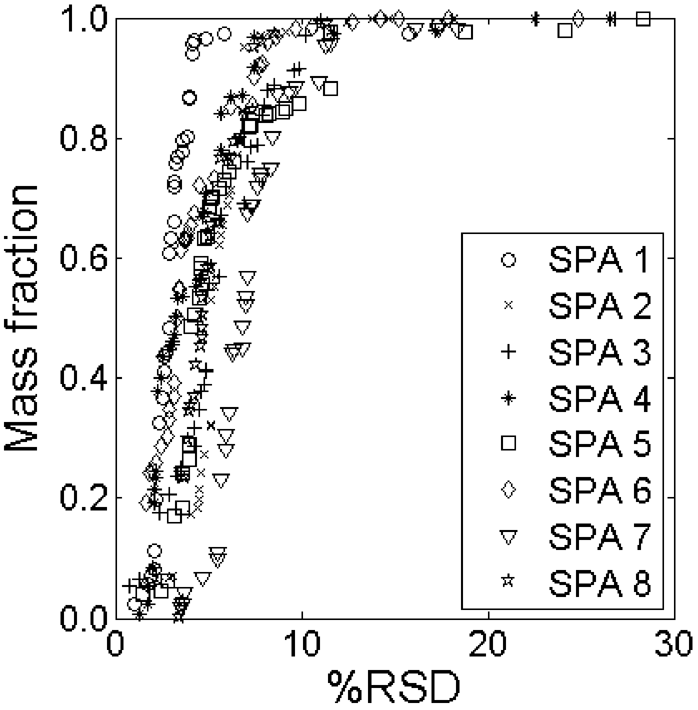

Figure 18: Cumulative mass fraction as function of %RSD.

Figure 19 shows more detailed profiles of the two measurements at the extreme ends, that is, SPA 1 and SPA 7, as well as that of the intermediate measurement, SPA 2. Similar data were added from a GC calibration standard to depict a “best case” measurement. The %RSD of the GC varies slightly over time, but is significantly lower than the %RSD obtained for all the collected samples. This indicates the potential for further improvements of the method. It is not clear whether the difference in repeatability between the three samples is the result of a fluctuating gasification process, incorrect sample collection or an error in the analysis. However, the similarity of the curve shapes implies that the error affects to the same extent all of the groups in a sample. An error induced within the elution or analysis would almost certainly affect the volatile species differently than it would the heavier species. Therefore, the difference in repeatability between the measurements is most likely related to the gasifier or the sample collection.

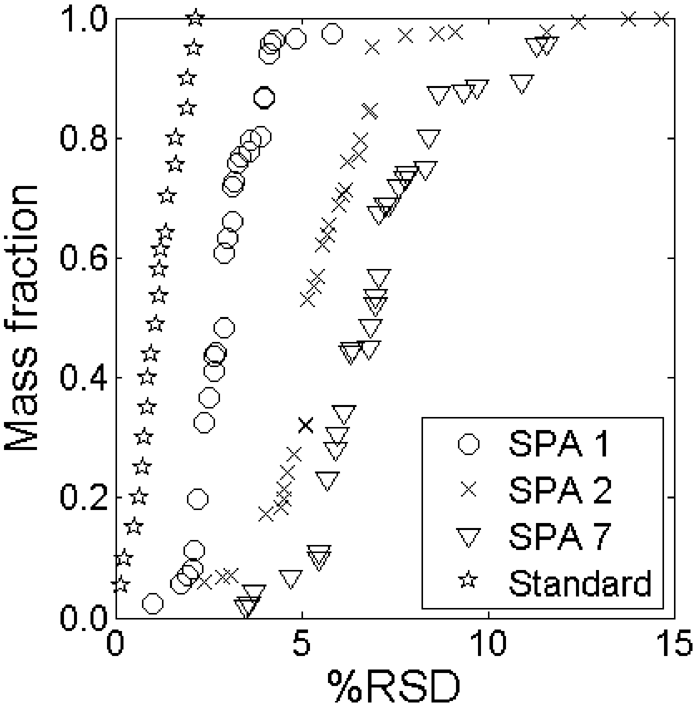

Figure 19: Cumulative mass fraction as function of %RSD.

The GC analysis method was designed to allow the detection of species within the boiling-point ranges of benzene to coronene. However, in all the measurements performed, only minor amounts of heavier tar components were detected, and coronene was not found in any sample (Figure 20). Initially, it was suspected that the heavier tars might have condensed on the filter or gas line. However, measurements performed on samples before the filter did not produce different results. Furthermore, from the time of their construction, the gasifier and sampling system have undergone more than 1000 h of operation at 350 °C, without any signs of fouling or blockage in the equipment. Therefore, it was concluded that the current measurements relate to the heavy end of the tar spectrum produced in the Chalmers gasifier.

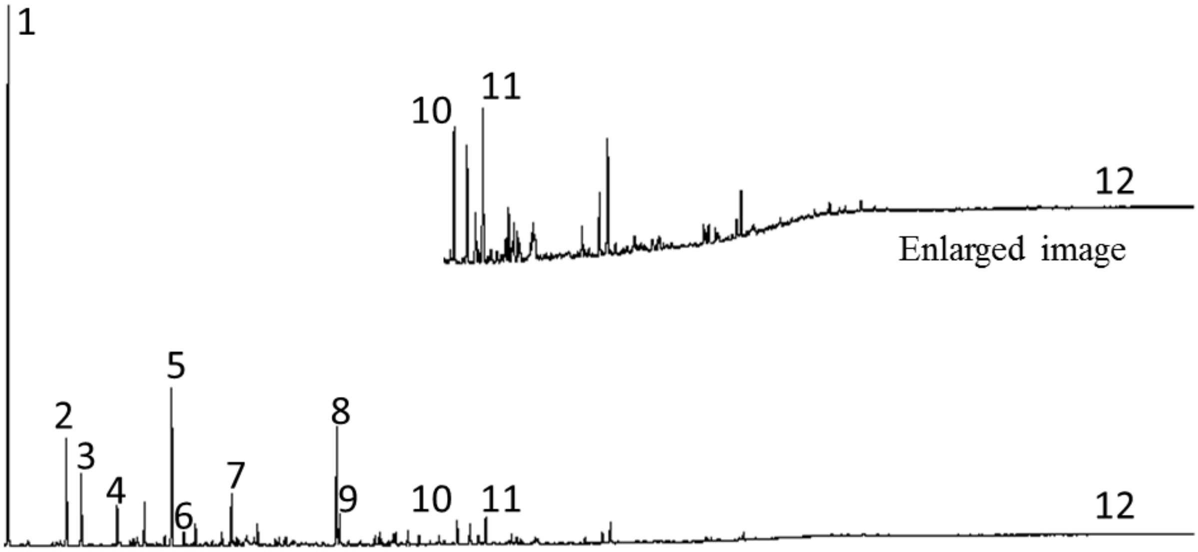

Figure 20: Segment of a chromatogram displaying the following peaks: 1, naphthalene; 2, 2-methylnaphthalene; 3, 1-methylnaphthalene; 4, biphenyl; 5, acenaphthylene; 6, acenaphthene; 7, fluorene; 8, phenanthrene; 9, anthracene; 10, fluoranthene; 11, pyrene; and 12, coronene.

4.4 High-Temperature Reactor

Synthetic gas measurements were performed on a known gas mixture to determine the degree of conversion, as well as the levels of accuracy and soot formation as a function of temperature. The average values obtained from the synthetic gas measurements performed at 1700 °C are presented in Table 2, together with the composition of the synthetic gas mixture. A sufficient conversion of large species was obtained, with only trace levels of CH_4 and C_2H_4 exiting the reactor system. Furthermore, the total volume of dry gas was increased by a factor of 1.82, as determined by the concentration of helium, due to the cracking of larger molecules and the water−gas shift reaction.

The concentration of nitrogen is not affected to the same extent due to an exchange of gas between the measured gas and the volumes that were purged with nitrogen prior to the measurement. However, this exchange of gas is small at <1 vol % of the flow exiting the reactor. After the publication of paper 4, the pack box (6) in Figure 10 was redesigned, resulting in significantly lower levels of gas exchange between the reactor and oven.

Table 2: Compositions of the inlet and outlet streams during synthetic gas HTR experiments conducted at 1700°C.

Species	H_2	CO	CO_2	CH_4	C_2H_2	C_2H_4	C_3H_8	He	N_2
Feed gas [vol%]	25.2	39.52	8.94	11.9	0.496	4.99	0.994	4.97	2.99
Exiting gas [vol%]	54.31	29.13	11.45	0.05	N.D.	0.03	N.D.	2.73	2.30

N.D. not detected

The soot yields from the validation experiments are presented in Figure 21, expressed as fractions of the supplied carbon [mass %]. The amount of soot collected after the HTR is shown as a function of the reactor temperature during operation at 1500, 1600, and 1700°C. There is a clear trend toward significant yields of soot at operating temperatures below 1700°C. The level of soot formation within the HTR is, most likely, much higher than the measured yields. Therefore, the difference between the measured points is more dependent upon the gasification of formed soot than differences in soot formation. This emphasizes the need for rapid transport to the hot zone of the reactor, via the narrow tube shown in Figure 10, so as to avoid the attachment of soot to the walls in regions that are too cold to support soot gasification.

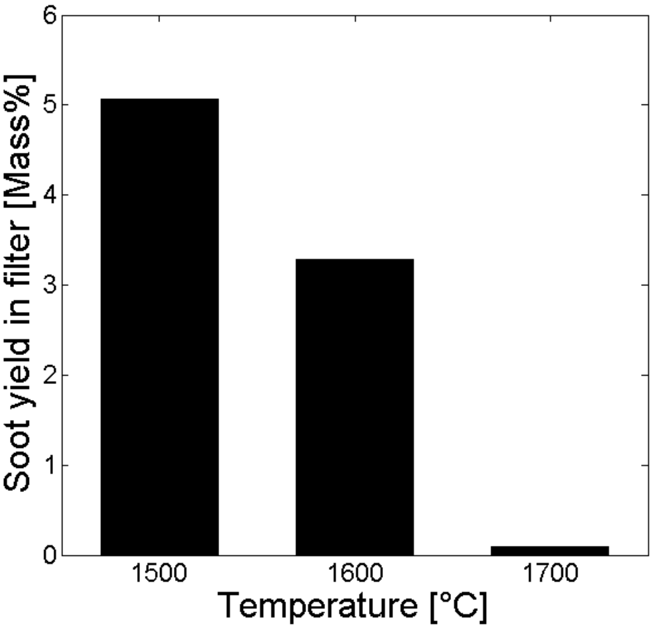

Figure 21: Yields of soot [mass %], for the validation experiments, collected in the filter as a function of temperature in the HTR at 1500, 1600, and 1700 °C.

The elemental yields and estimated errors of analysis for the validation experiments are reported in Paper 4 and are summarized as follows. The measured carbon yield in the reformed gas corresponds to 99.83% of the carbon in the synthetic gas, which is within the error of the employed analysis equipment. Furthermore, the amount of carbon recovered as soot in the DPF was 0.09% of the supplied carbon at 1700°C, which agrees well with the determined gas yield. The determined dry gas yields of oxygen and hydrogen are both significantly higher than 100% due to the water-gas-shift reaction. Consequently, it is not possible to determine their individual errors, in terms of yields, without an accurate steam measurement. However, as shown in Paper 4, the combined effect of these two errors can be determined by quantifying the oxygen addition. The determined error in oxygen addition was 2.8% of the oxygen supplied in the synthetic gas, indicating a significant level of added oxygen in the HTR. This could be caused by inward air leakages, the presence of pockets of air inside the reactor system, or outward leakage of hydrogen. To determine the actual cause, accurate measurements of the steam before and after the reactor are needed, which would allow individual quantification of the levels of hydrogen and oxygen. However, the accuracy of the oxygen addition in Paper 4 is limited to that of the reactor system.

4.4.1 Applied Measurements

The high-temperature reactor system was used in combination with the gas conditioning system (Figure 7) to perform measurements in the Chalmers DFB gasifier.

The average concentrations [vol %] of the species exiting the HTR are shown in Table 3, together with the concentrations of the species in the cold gas. The results show a very high degree of conversion of hydrocarbons heavier than methane, the level of which was close to the detection limit of the method. Furthermore, the level of tar exiting the HTR, as measured using the SPA method, was negligible compared to the background noise of the analysis.

Comparing the nitrogen concentrations in the two systems, it becomes evident that there was an inward leakage of air prior to the HTR. However, the use of two parallel measurement systems for the HTR gas and the cold gas enables quantification of the leaked air. Thus, the leak can be compensated for in the subsequent calculations. The nitrogen in the cold gas is supplied by the fuel feeding system and is compensated for in a similar way.

Table 3: Levels of components of the cold gas and HTR gas from measurements performed in the DFB gasifier.

Species	H_2	CO	CO_2	CH_4	C_2H_2	C_2H_4	C_2H_6	C_3H_6	He	N_2	H_2S
Cold gas [vol%]	32.21	19.57	29.55	8.31	0.11	2.51	0.43	0.25	1.07	5.37	0.61
HTR gas [vol%]	46.01	32.06	13.70	0.02	N.D.	N.D.	N.D.	N.D.	0.66	7.55	N.D.

N.D. not detected

The measured amounts of carbon, relative to the levels in the fuel feed, after the HTR and the gas-conditioning system are shown in Figure 22 for nine measured points. The difference in carbon yield between the two measurements reflects the amount of carbon present in the condensable species, as calculated using Eq 3 and indicated by the double-arrow in the Figure.

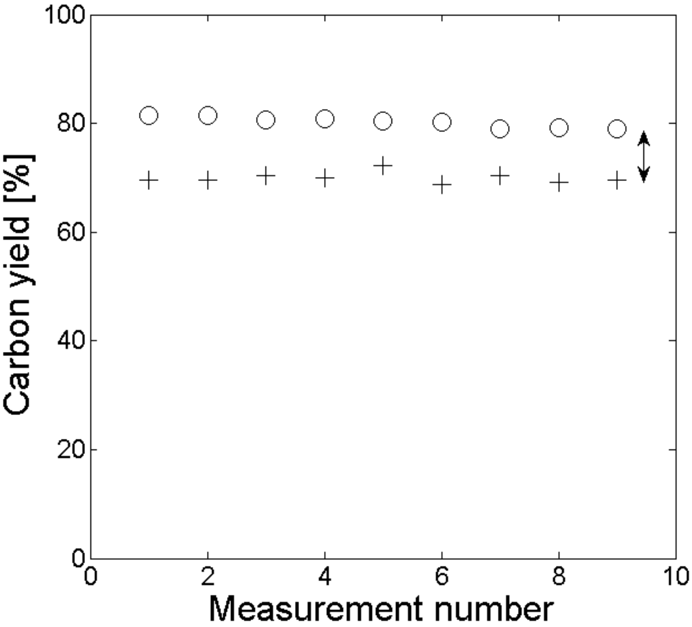

Figure 22: Relative carbon yields in the cold gas (+) and HTR gas (o).

The average concentration of condensable species, expressed as a function of the H/C ratio is depicted in Figure 23 as a solid line starting at CH_{min}, together with the H/C ratio and concentration of tar measured by SPA. The graph also contains the CH_{min} value and concentration of the unidentified condensable species, obtained by subtracting the SPA tar level from the average level of condensable species. The dotted lines represent the standard deviation of the analysis. The H/C and O/C ratios for the total condensable species increase from the CH_{min} value and zero, respectively, owing to the addition of water (Figure 24) according to Eq 4. As seen in Figure 23, the concentration of unidentified condensable species, at CH_{min}, is more than twice that of the measured tar, using the SPA method. This shows the importance of fulfilling the mass balance of the system as roughly 6% of the carbon content in the provided fuel is found as unidentified species. In line with the tar measurement of Figure 20, only minor amounts of heavy tar species where detected in the performed SPA measurements. This indicates that the H/C and O/C ratios of the unidentified species are significantly higher than CH_{min} and zero, respectively, in accordance with species lighter than benzene.

Measurements of the incoming steam and the condensate in the raw gas would enable determinations of the H/C ratio and corresponding O/C ratio of the condensable species. However, the amount of water needed to increase the H/C ratio from the CH_{min} (0.83) to 1.5 is less than 3 mass % of all incoming steam. Therefore, the mass balance of water in the gasifier system needs to be determined with a high accuracy to yield useful information concerning the H and O content of the condensable species. Nevertheless, as the condensable compounds contain little water, their effect on the raw gas concentration of the steam is negligible. Consequently, the concentration of steam can be calculated using data on the flow and composition of the cold gas, the condensable compounds described by CH_{min}, and the steam input to the gasifier. An average tar molecule is chosen to determine the volumetric flow of condensable compounds, in this case, benzene. Furthermore, if the steam input is not known, it can be derived by comparing the cold gas with the wet gas exiting the HTR.

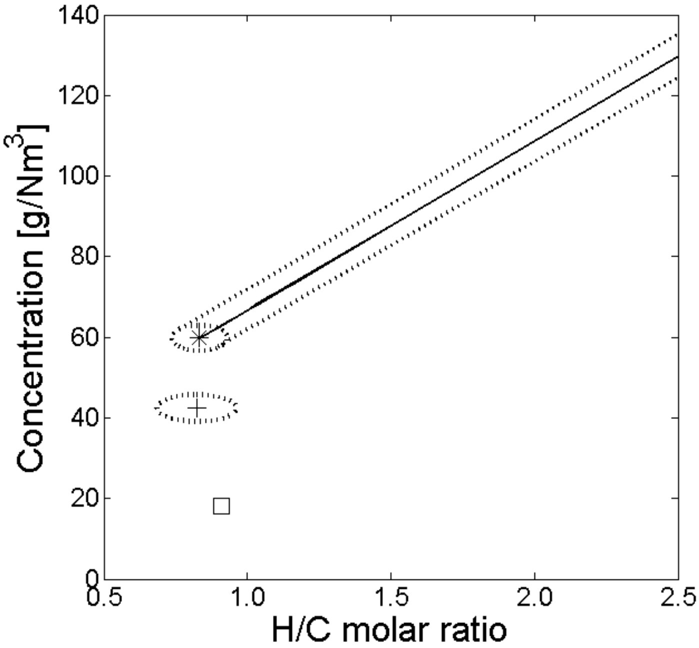

Figure 23: Concentrations, as a function of the H/C ratio of condensable species (∗), of unidentified species (+) at the CH_{min}, and for the SPA-analyzed tar (□).

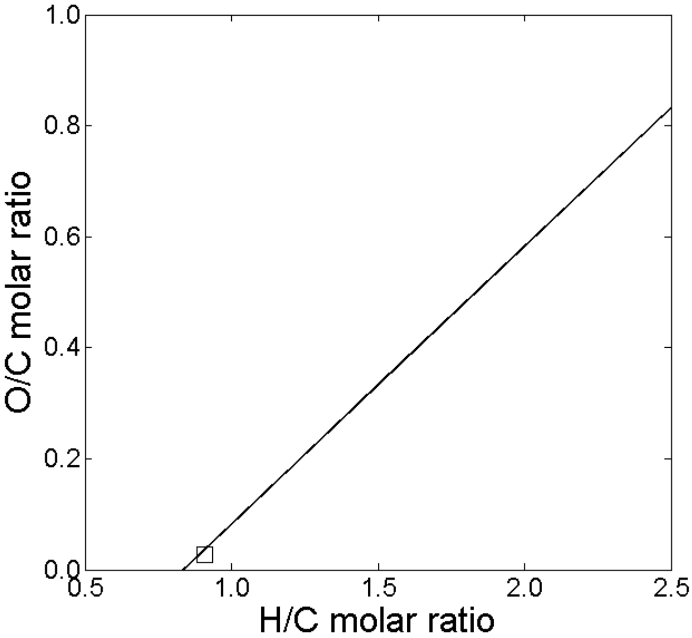

Figure 24: O/C ratio as a function of the H/C ratio for the condensable species and SPA-analyzed tar (□).

The ability to determine precisely the H/C and O/C ratios of the condensable compounds is of great value, as it generates information concerning the true concentration and, possibly, the size range and boiling point of the unidentified species. However, the energy content can be determined without this information, provided that the carbon flows and CH_{min} are known. The calculated cold gas, raw gas, and theoretical raw gas efficiencies were 61.4%, 73.5%, and 81.8%, respectively, and the raw gas LHV was 7.11 MJ/Nm3, according to eqs 8−10. Consequently, 12.1% of the energy in the fuel was found in the condensable species. This corresponds well to data presented in previous studies[35], which ranges from around 20% for pyrolysis to 10−15% for DFB gasification with sand. Furthermore, the carbon yield of the condensable species, presented in Figure 22, corresponds to roughly 10% of the carbon content of the fuel or 5 mass % of the dry fuel feed. This agrees well with presented data for fluidized bed gasifiers[2].

If a gas-conditioning system is not available, the raw gas LHV can be estimated using only the data obtained from the HTR system. In Figure 25, the calculated equivalent LHVs of the wet raw gas, as well as the LHV of the wet HTR gas, are shown relative to the measured LHV for the wet raw gas. The measured values of the raw and HTR gas LHVs fall within the interval of maximum hydrogen and methane yields. Furthermore, the methane-equivalent LHV differs from the measured value by 1.3%. The other equivalent species, from ethane to acetylene, overestimate the heating value for the produced gas.

As previously mentioned, different process types will have different optimal equivalent species. For example, high-temperature gasification for syngas production would be best described using an equivalent syngas mixture that lies somewhere between the maximum theoretical yields of H_2 and CO. Similarly, the DFB gasification measurements performed in the present study reveal good agreement with the methane-equivalent heating value.

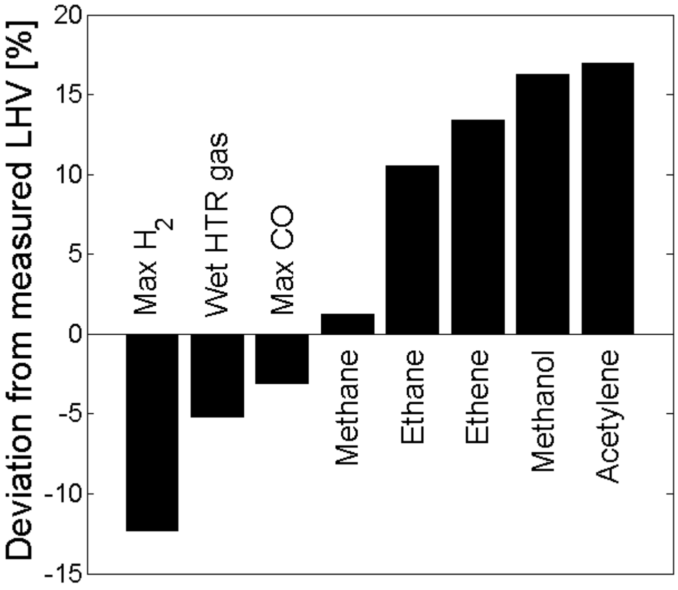

Figure 25: Deviations in the calculated LHVs of the wet raw gas compared to the measured LHVs of the wet raw gas for HTR gas and equivalent gases and gas mixtures.

5 - Conclusions

5.1 Primary and Secondary Measures for Tar Reduction

The effects of catalytic bed materials on the tar evolution were compared by implementing ilmenite ore in the Chalmers DFB gasifier and manganese ore in a chemical looping reactor (CLR).

Both approaches resulted in significantly decreased levels of tar, around 50% at optimal conditions. The change in tar composition over the CLR followed the expected trends of tar maturation, resulting in increased amounts of naphthalene and larger aromatic species. The change in tar composition from the gasifier measurements differed significantly from that of the CLR. At low fluidization, the yields of all tar groups were decreased and, at higher levels of fluidization, the yields of both phenols and heavy species were least affected. From these measurements, it is evident that the manner of catalyst implementation can greatly influence its performance.

When comparing the gas composition in terms of the syngas components CO, CO_2, and H_2 between the CLR and gasifier measurements, a higher degree of oxygen transport is apparent in the gasifier. This is because the bed material flow is determined by the heat demand of the gasifier and, as a result, it cannot be manipulated to minimize the oxygen transport. The heat demand of the CLR is much less than that of the gasifier, resulting in a much higher potential for the optimization of the oxygen transport.

5.2 Measurement Techniques

Two different methods of analysis were investigated for tar analysis and the elemental quantification of the raw gas.

The SPA method for measurement of tar species was evaluated in terms of detection limits and reproducibility. A majority of the mass of the collected samples was quantified with a relative standard deviation well within 10%. However, the absorption of lighter species, ranging from benzene to xylene, was insufficient using the employed column. Since the publication of Paper 3, the elution method for the collected samples has been revised to contain fewer steps and chemicals. Furthermore, new sample extraction columns, containing an additional bed of active carbon, are being used to quantify, with accuracy, the lighter tar species.

The high-temperature reactor, developed for total elemental quantification of the raw gas, was evaluated in validation experiments. The determined carbon yield and soot formation values were within the margin of error of the analysis. The measured error for the oxygen addition was higher than the error of analysis and corresponded to 2.8% of the oxygen provided in the dry synthetic gas mixture. The reactor was rebuilt after the publication of Paper 4 and there are currently no signs of any significant effects of internal gas exchange. However, further measurements are needed for verification.

Online measurements of the Chalmers DFB gasifier enabled indirect determinations of the oxygen transport, the total carbon conversion in the gasifier, and the amount of condensable carbon, using mass balance calculations. Measurements performed after the high-temperature reactor validated near-complete conversion of all tar components, as well as of the micro-GC-detectable hydrocarbons of larger mass than methane. Recent measurements include the diesel particulate filter, for soot quantification, after the high-temperature reactor to allow semi-continuous monitoring of the reactor performance. Furthermore, as any potential soot formation can be quantified, this measurement can be used to correct the total error in the carbon quantification.

The performed measurements were used to determine the lowest possible H/C ratio, CH_{min}, of the condensable species. This information, combined with a lack of heavy species being detected in the SPA samples, suggests that the unidentified condensable species have boiling points below that of benzene. Furthermore, the CH_{min} value and the average oxygen-based heating value were used to calculate the energy content of the condensable species. As a result, the wet raw gas efficiency could be determined and compared to the theoretical raw gas efficiency, providing the net enthalpy change within the gasifier.

Increasing the H/C ratio of the condensable species from the CH_{min} value to 1.5 would require less than 3% of the steam provided to the gasifier. Consequently, using CH_{min} to represent the condensable species induces only a small error in the water balance of the system. This allows calculation of the steam concentration and the corresponding LHV of the raw gas. Furthermore, the methane-equivalent heating value, determined using only data from the high-temperature reactor, was within 1.3% of the measured LHV in the present study.

6 - Future Work

The tools and methods, developed during this work, offer the possibility of accurately measuring the entire raw gas spectrum. At present, several opportunities for future work are available, in terms of improving both the measurement and the analysis of the results.

- As discussed in the Theory section of this thesis, a clear representation of all flows and species, in the raw gas, is required to construct a comprehensive model of the gas-phase reactions of a gasifier. Furthermore, a fulfilled mass balance is essential for the purposes of determining the extent of reactions such as the water-gas-shift reaction and the reformation or creation of tar species. Future measurements, performed in line with the work presented in this thesis, have the potential to distinguish the underlying reaction mechanisms related to the condensable species. Additionally, they will serve to indicate further improvements that can be made in terms of measurements.

- The heated raw gas filter is used to remove particulates from the raw gas prior to analysis by means of the gas conditioning system or the high temperature reactor. However, if there is soot formation within the gasifier, some fraction of the produced soot will, most likely, be able to by-pass the filter. This would not affect the measurement of the gas conditioning system. However, if soot enters the HTR and is converted, this would affect the determined amount of condensable species along with its CH_{min} value. Consequently, investigations are needed to determine if soot can enter the HTR, as well as how to avoid it in future measurements.

7 - References

---

1. Higman, C. and M. Van der Burgt, *Gasification*. 2011: Gulf professional publishing.
2. Milne, T.A., N. Abatzoglou, and R.J. Evans, *Biomass gasifier" tars": their nature, formation, and conversion*. 1998: National Renewable Energy Laboratory Golden, CO.
3. Rauch, R., et al., *Comparison of different olivines for biomass steam gasification*. 2004: na.
4. Grootjes, A., et al., *Improved Gasifier availability with bed material and additives.* 2013.
5. Bergman, P.C., S.V. van Paasen, and H. Boerrigter. *The novel "OLGA" technology for complete tar removal from biomass producer gas*. in *Pyrolysis and Gasification of Biomass and Waste, Expert Meeting, Strasbourg, France*. 2002.
6. Dayton, D., *A review of the literature on catalytic biomass tar destruction.* NREL Report, NREL/TP-510-32815, NREL, Golden, CO, 2002.
7. Lind, F., M. Seemann, and H. Thunman, *Continuous catalytic tar reforming of biomass derived raw gas with simultaneous catalyst regeneration.* Industrial & Engineering Chemistry Research, 2011. 50(20): p. 11553-11562.
8. Lyngfelt, A., B. Leckner, and T. Mattisson, *A fluidized-bed combustion process with inherent CO_2 separation; application of chemical-looping combustion.* Chemical Engineering Science, 2001. 56(10): p. 3101-3113.
9. Ahmadi, M., et al., *Development of an on-line tar measurement method based on photo ionization technique.* Catalysis Today, 2011. 176(1): p. 250-252.
10. Meng, X., et al., *Tar formation in a steam-O_2 blown CFB gasifier and a steam blown PBFB gasifier (BabyHPR): Comparison between different on-line measurement techniques and the off-line SPA sampling and analysis method.* Fuel Processing Technology, 2012. 100: p. 16-29.
11. Mitsakis, P., et al., *Optical measurement of tars in a fluidized bed gasifier: influence of fuel type and gasification parameters on their formation.* Biomass Conversion and Biorefinery, 2013: p. 1-11.
12. Moersch, O., H. Spliethoff, and K. Hein, *Tar quantification with a new online analyzing method.* Biomass and Bioenergy, 2000. 18(1): p. 79-86.
13. Patuzzi, F., et al., *A comparison between on-line and off-line tar analysis methods applied to common reed pyrolysis.* Fuel, 2013.
14. Neeft, J., et al., *Guideline for sampling and analysis of tars and particles in biomass producer gases.*
15. Brage, C., et al., *Use of amino phase adsorbent for biomass tar sampling and separation.* Fuel, 1997. 76(2): p. 137-142.

16. Osipovs, S., *Comparison of efficiency of two methods for tar sampling in the syngas.* Fuel, 2013. 103: p. 387-392.
17. Israelsson, M., M. Seemann, and H. Thunman, *Assessment of the Solid-Phase Adsorption method for sampling biomass-derived tar in industrial environments.* Energy & Fuels, 2013. 27(12): p. 7569-7578.
18. Neves, D., et al., *Method for online measurement of the CHON composition of raw gas from biomass gasifier.* Applied Energy, 2014. 113: p. 932-945.
19. Font Palma, C., *Model for biomass gasification including tar formation and evolution.* Energy & Fuels, 2013. 27(5): p. 2693-2702.
20. Morf, P., P. Hasler, and T. Nussbaumer, *Mechanisms and kinetics of homogeneous secondary reactions of tar from continuous pyrolysis of wood chips.* Fuel, 2002. 81(7): p. 843-853.
21. Su, Y., et al., *Experimental and numerical investigation of tar destruction under partial oxidation environment.* Fuel Processing Technology, 2011. 92(8): p. 1513-1524.
22. Corella, J., et al., *Two advanced models for the kinetics of the variation of the tar composition in its catalytic elimination in biomass gasification.* Industrial & engineering chemistry research, 2003. 42(13): p. 3001-3011.
23. Bruinsma, O.S., et al., *Gas phase pyrolysis of coal-related aromatic compounds in a coiled tube flow reactor: 1. Benzene and derivatives.* Fuel, 1988. 67(3): p. 327-333.
24. Bruinsma, O.S., et al., *Gas phase pyrolysis of coal-related aromatic compounds in a coiled tube flow reactor: 2. Heterocyclic compounds, their benzo and dibenzo derivatives.* Fuel, 1988. 67(3): p. 334-340.
25. Jess, A., *Mechanisms and kinetics of thermal reactions of aromatic hydrocarbons from pyrolysis of solid fuels.* Fuel, 1996. 75(12): p. 1441-1448.
26. Evans, R.J. and T.A. Milne, *Molecular characterization of the pyrolysis of biomass.* Energy & Fuels, 1987. 1(2): p. 123-137.
27. Evans, R.J. and T.A. Milne, *Molecular characterization of the pyrolysis of biomass. 2. Applications.* Energy & fuels, 1987. 1(4): p. 311-319.
28. Gerun, L., et al., *Numerical investigation of the partial oxidation in a two-stage downdraft gasifier.* Fuel, 2008. 87(7): p. 1383-1393.
29. Kiel, J., et al., *Primary measures to reduce tar formation in fluidised-bed biomass gasifiers.* ECN, ECN-C-04-014, 2004.
30. Williams, P.T. and D.T. Taylor, *Aromatization of tyre pyrolysis oil to yield polycyclic aromatic hydrocarbons.* Fuel, 1993. 72(11): p. 1469-1474.
31. Fuentes-Cano, D., et al., *The influence of temperature and steam on the yields of tar and light hydrocarbon compounds during devolatilization of dried sewage sludge in a fluidized bed.* Fuel, 2013. 108: p. 341-350.
32. Cypres, R., *Aromatic hydrocarbons formation during coal pyrolysis.* Fuel Processing Technology, 1987. 15: p. 1-15.
33. Fitzpatrick, E., et al., *Mechanistic aspects of soot formation from the combustion of pine wood.* Energy & Fuels, 2008. 22(6): p. 3771-3778.
34. Scott, D. and J. Piskorz, *The flash pyrolysis of aspen-poplar wood.* The Canadian Journal of Chemical Engineering, 1982. 60(5): p. 666-674.
35. Larsson, A., et al., *Evaluation of Performance of Industrial-Scale Dual Fluidized Bed Gasifiers Using the Chalmers 2–4-MWth Gasifier.* Energy & Fuels, 2013.
36. Kaufman Rechulski, M., et al., *Liquid-Quench Sampling System for the Analysis of Gas Streams from Biomass Gasification Processes. Part 2: Sampling Condensable Compounds.* Energy & Fuels, 2012. 26(10): p. 6358-6365.

37. Osipovs, S., *Sampling of benzene in tar matrices from biomass gasification using two different solid-phase sorbents.* Analytical and Bioanalytical Chemistry, 2008. 391(4): p. 1409-1417.
38. Min, Z., et al., *Catalytic reforming of tar during gasification. Part I. Steam reforming of biomass tar using ilmenite as a catalyst.* Fuel, 2011. 90(5): p. 1847-1854.